RESPONSE OF EXTENDED EULER-BERNOULLI BEAM UNDER IMPULSE LOAD USING WAVELET SPECTRAL FINITE ELEMENT METHOD

A THESIS

submitted by

MALLIKARJUN B

for the award of the degree

of

MASTER OF TECHNOLOGY

STRUCTURAL ENGINEERING DIVISION
DEPARTMENT OF CIVIL ENGINEERING
NATIONAL INSTITUTE OF TECHNOLOGY, ROURKELA 769008

May 2012

NATIONAL INSTITUTE OF TECHNOLOGY
ROURKELA – 769008, ORISSA
INDIA

CERTIFICATE

This is to certify that the thesis entitled **"RESPONSE OF EXTENDED EULER-BERNOULLI BEAM UNDER IMPULSE LOAD USING WAVELET SPECTRAL FINITE ELEMENT METHOD"** submitted by **Mallikarjun B** in partial fulfillment of the requirement for the award of **Master of Technology** degree in **Civil Engineering** with specialization in **Structural Engineering** to the National Institute of Technology, Rourkela is an authentic record of research work carried out by him under my supervision. The contents of this thesis, in full or in parts, have not been submitted to any other Institute or University for the award of any degree or diploma.

Project Guide

Rourkela-769 008

Date:

Dr. Manoranjan Barik
Associate Professor
Department of Civil Engineering

ACKNOWLEDGEMENTS

First and foremost, praise and thanks goes to my God for the blessing that has been bestowed upon me in all my endeavors.

I am deeply indebted to **Dr. Manoranjan Barik,** Associate Professor, my advisor and guide, for the motivation, guidance, tutelage and patience throughout the research work. I appreciate his broad range of expertise and attention to detail, as well as the constant encouragement he has given me over the years. There is no need to mention that a big part of this thesis is the result of joint work with him, without which the completion of the work would have been impossible.

I extend my sincere thanks to the Head of the Civil Engg Department **Prof. N. Roy**, for his advice and unyielding support over the year.

The personal communication and discussion with **Dr. Mira Mitra of** Indian Institute of Technology, Bombay is of immense help. Her valuable suggestions and timely co-operation during the project work is highly acknowledged. The author extends his heartfelt thanks to her.

I would like to take this opportunity to thank my Parents and my sister for their unconditional love, moral support, and encouragement for the timely completion of this project.

I am grateful for friendly atmosphere of the Structural Engineering Division and all kind and helpful professors that I have met during my course.

I express my most sincere admiration to my friends, (in no particular order) **Bijily B**., **Suji P**, **Venkateshwara Reddy** and to all my classmates for their cheering up ability which made this project work smooth.

So many people have contributed to my thesis, my education, and it is with great pleasure to take the opportunity to thank them. I apologize, if I have forgotten anyone.

Mallikarjun B

Roll No: 210ce2022

M.Tech (Structures)

PREFACE

Transform methods are some of those methods which are able to solve certain difficult ordinary and partial differential equation. The most commonly used transform for these solutions are Laplace and Fourier transforms. Wavelet transforms are new entrants in to this area, although they are quite popular with electrical and communication engineers in characterizing and synthesizing the time signals. The utility of wavelet transforms is shown in structural engineering by addressing problems involving solutions of ordinary and partial differential equations encountered in dynamical related problems.

Dynamical problems in structural engineering fall under two categories, one involving low frequencies, which is called structural dynamics problems, and the other involving very high frequencies, which is called the wave propagation problems. The most problems in structural engineering fall under the former category, wherein the response of the entire structural system is characterized using only the first few vibrational modes. The wave propagation is a multi-modal phenomenon involving vibrational modes of very high frequencies. Conventional analysis tools such as finite element cannot handle these problems due to modeling limitations and extensive computational cost. The only alternative to such problems is the method based on transforms.

Spectral finite element (SFE) method is one such transform method, which can be a viable alternative to solving problems involving high frequency excitations. SFE based on Fourier transform is quite well known and established. However, it has severe limitations in handling finite structures and specifying non-zero boundary/initial conditions, and thus its utility in solving real world problems involving high frequency excitation is limited.

The aim of the present work is to show that the wavelet transform is very useful in solving ordinary differential equations by modeling the structure as a discrete system involving structural dynamic problems and it is to use wavelet transform to solve those problems involving partial differential equations. In this work, the response of an cantilever Extended Euler-Bernoulli aluminum beam under impulse load applied axial and transverse at the free end is shown. The response is being obtained by coding programs in MATLAB.

Contents

List of Figures

List of Tables

List of symbols

Although all the principle symbols used in this thesis are defined in the text as they occur, a list of them is presented below for easy reference. On some occasions, a single symbol is used for different meanings depending on the context and thus its uniqueness is lost. The contextual explanations of the symbol as its appropriate place of use is hoped to eliminate the confusion.

English

a, b, and c	material constants
A	cross sectional area
a_k	filter coefficients
A_n	incident wave coefficient
B	filter coefficient matrix
B	width of Extended Euler-Bernoulli beam
D	depth of Extended Euler-Bernoulli beam
L	length of Extended Euler-Bernoulli beam
B_n	reflected wave coefficient
$\mathrm{C_p}$	Phase speed
$\mathrm{C_g}$	group speed
$c_{j,k}$	approximation coefficients
$[C]$	dampimg matrix
c_l	constant coefficients
D	Daubechies
$d_{j,k}$	detail coefficients
db	Daubechies wavelet
E	Young's modulus
F	applied axial force
F(t)	Impulse load
I	moment of inertia

I	Complex $\sqrt{-1}$
J	dilation indices
k	wave number
[k]	stiffness matrix
$[\hat{k}_e]$	elemental dynamic stiffness matrix
M	vanishing moments
$[M]$	global mass
N	Order of Daubechies
n	Sampling points
p	polynomial of order
$\hat{F}(x)$	nodal force
$\hat{V}(x)$	nodal shear force
$\hat{M}(x)$	nodal moment
[R]	amplitude ratio matrix
T	total period
t	time
$u(x,t)$	axial diaplacement
$\{\ddot{u}\}$	acceleration
$\{\dot{u}\}$	velocity
$\{u\}$	displacement
$\{\hat{U}\}$	nodal displacement vector
x	spatial coordinates
xs	arbitrary points
$w(x,t)$	tranverse displacment

Greek

ω_n	circular frequency
Δt	time interval between two sampling points.
$\psi(t)$	wavelet function or mother wavelet
$\varphi(t)$	scaling function or father wavelet
φ'	first derivative of scaling function
φ''	second derivative of scaling function
Ω_{j-k}^{1}	first order connection coefficients
Ω_{j-k}^{2}	second order connection coefficients
Γ^1	first order connection coefficient matrices.
Γ^2	second order connection coefficient matrices.
Φ	eigenvector matrix of Γ^1
Π	diagonal matrix containing corresponding eigenvalues λ_j.
Π^2	diagonal matrix with diagonal terms λ_j^2
$[\Theta]$	diagonal matrix with diagonal terms
μ_i^j	Moment of scaling functions
ω_t	frequency of transition
$\omega_{cut-off}$	cut off frequency
η	dampimg ratio
ρ	density of material

CHAPTER ~ 1

Introduction

1.1 Overview

Wavelets are effectively used for signal processing and solution of differential equations. Wavelet transform is implemented to solve and analyze problems associated with engineering mechanics. The use of wavelets in mechanics can be viewed from different perspectives, such as the analysis of mechanical responses for extraction of model parameters, de-noising, damage measures etc. the solution of the differential equations governing the mechanical system; the solution of structural dynamics and wave propagation problems using wavelet transform methods.

Structural dynamics deal with lower frequencies in the magnitude of a few hundred Hertz, or only the first few modes of vibrations and involve the study of steady state response. On the other hand, wave propagation results from high frequency excitations, in the order of Kilohertz and involves the study of transient response.

1.1.1 Solution methods for structural dynamics problems

The solution of structural dynamics problems can either be the determination of system parameters, mostly, natural frequencies and mode shapes, or simulations of the response of the system to external excitations such as initial displacements, external load, support motion etc. For a discrete system, i.e. a multi-degree of freedom (MDOF) system, the governing equations (ODEs) are coupled in general.

Apart from wavelet analysis of structural dynamics, this mainly concentrates on wavelet-based spectral analysis of wave propagation. A numerical scheme called wavelet-based spectral finite element method is implemented for modeling of an Extended Euler-Bernoulli beam. This technique helps the computational efficiency of spectral analysis while possessing several

advantages over Fourier transform-based spectral analysis particularly for capturing near field phenomena.

1.1.2 Solution Methods for Wave Propagation Problems

Wave propagation is a transient dynamic phenomenon resulting from short duration loading. Such transient loadings have high frequency content. The main difference between the structural dynamics and wave propagation in structures arises due to high frequency excitations. Structures very often experience such loadings in forms of impact and blast loadings like gust, bird hit, tool drops etc. Apart from understanding the behavior of structures under such loadings, wave propagation analysis is also important to gain knowledge about their high frequency characteristics which have several applications. The applications include structural health monitoring using diagnostic waves and control of wave transmission for reduction of noise and vibration.

Though finite element (FE) method is versatile and widely used to model complex structures for structural dynamics problem, it is highly unsuited for wave propagation analysis. Higher frequency content of the loading in wave propagation problems requires very fine mesh with the element size comparable to the wave lengths, which are very small at higher frequencies. This results in large system size and huge computational cost. In addition to the fine mesh, to obtain system response, the mode superposition method or time integration schemes have to be implemented after FE modeling. Mode superposition method cannot be applied for wave propagation analysis. This is because for such problems the model parameters have to be extracted over a wide range of frequency. This has to be done through eigen value analysis which is computationally very expensive. Alternatively there are several time integration schemes used for solution of dynamic problems. These schemes can be used for simulation of

wave response. In these methods, analysis is performed over a small time step, which is a fraction of the total time for which the response histories are required. For some time integrations schemes, however, a constraint is placed on the time step, and this coupled with large system sizes makes the FE solution of wave propagation problems computationally prohibitive. The alternative numerical techniques are adopted for these problems and several such techniques are Boundary Element Method (BEM) [7, 41], discontinuous Galerkin method [61, 24], Mesh less Local Petrov-Galerkin (MLPG) method [8], wave finite element method [65] etc.

Among these techniques, many methods are based on integral transform [18] which include Laplace transform, Fourier transform, and most recently wavelet transform. In these methods, first the governing equations are transformed to the frequency domain using the forward transform in time. Such transformation reduces the governing PDEs by one dimension to differential equations with only spatial variations. The solution of these transformed equations is much easier than the original PDEs and often has analytical solution. These solutions in transformed frequency domain contain information of several frequency dependent wave properties essential for the analysis. The time domain solution is then obtained through inverse transform. The use of Laplace transform for solution of wave equation has been limited because of the difficulty in performing the inverse transform. On the other hand, the application of continuous Fourier transform (CFT) for such purpose has been reported [63], but even here, the inverse transform required is difficult to obtain and, these methods are suited only for far-field behavior like seismological studies.

In structural wave propagation, the structures are finite, and hence these schemes are not adequate since due to inherent problems in obtaining the transform, it cannot provide information about the reflection of waves on interaction between different boundaries and discontinuities.

The forward and inverse discrete Fourier transform (DFT), however can be numerically implemented. Fast Fourier transform (FFT) is the easy and fast algorithm for DFT. Spectral finite element (SFE) is one such method on Fourier transform and initially proposed by Narayanan and Beskos [59] and popularized by Doyle and his co-researchers [16]. In SFE, the differential equations are reduced to ODEs using Fourier transform in time. The solution gives the transformed displacements, which are converted to the displacements in time domain through inverse transform. The SFE technique like the other integral transform-based methods is effective in handling inverse problems like force identification and system identification.

From the mathematical explanation of wavelets, the wavelets are potential for spectral finite element formulation. There are several wavelets like Daubechies orthogonal wavelets, bi-orthogonal spline (B-spline) wavelets, interpolation wavelets, which have compactly supported bases with local supports and orthogonal properties. Thus they can be used to solve partial differential wave equations through integral transform because of the following advantages. Firstly, wavelet allows finite domain analysis and imposition of initial or boundary conditions which are possible due to the local support of these basis functions. Secondly, these bases are bounded both in time and frequency domains. However, the resolution in frequency domain may be reduced when compared to Fourier transform-based SFE and this is the trade-off to obtain better resolution in time domain analysis.

Wavelets have several encouraging properties for their use in numerical solution of partial differential equations (PDEs). The researchers [1, 20, 29, 17] have provided a review of wavelet techniques for solution of PDEs. The orthogonal, compactly supported wavelet basis of Daubechies [13, 15], exactly approximates polynomial of increasingly higher order. These wavelet bases can provide accurate and stable representation of differential operations even in

region of strong gradients or oscillations. In addition, it has the advantage of multi resolution analysis over the traditional methods. The main drawback of Fourier based spectral approach is that it cannot handle waveguide of short lengths. This is because, short lengths forces multiple reflections at smaller time scales. Since Fourier transforms are associated with a finite time window, shorter length of waveguide do not allow the response to die down within the chosen time window, irrespective of the type of damping used in modeling. These forces the response to wrap around, that is the remaining part of the response beyond the chosen time window, will start appearing first. This totally distorts the response. It is in such cases compactly supported wavelets, which have localized basis functions, can be efficiently used for waveguide of short lengths. Different wavelet based modeling techniques for simulations of wave propagation have been presented [25].

In the present work an approach similarly to SFEM is followed. Daubechies scaling functions are used for approximation in time and this reduces the PDE to ODEs in spatial dimension. These ODEs formed are coupled unlike those in FFT based SFEM (FSFEM). The system of coupled ODEs is decoupled performing an eigenvalue analysis, which decreases the computational cost considerably. The eigen analysis involved is time consuming, but this can be computed and stored as it is not related to the particular problem. The decoupled ODEs are then solved similarly as in SFEM and a wavelet based spectral element (WSFE) is formulated.

1.2 Numerical methods for solving PDEs

A brief introduction about some numerical methods to solve the PDEs

1.2.1 Finite difference method

Finite Difference Method (FDM) is most commonly used method to solve Ordinary Differential Equations (ODEs) and PDEs in a bounded domain. The basic idea of finite difference methods is simple: derivatives in differential equations are written in terms of discrete quantities of dependent and independent variables, resulting in simultaneous algebraic equations with all unknowns prescribed at discrete nodal points for the entire domain. For example, the order of convergence in second order FDM is ($N-2$) where N is number of nodal points. In brief about FDM, the different unknowns are defined by their values on discrete (finite) grid and differential operators are replaced by difference operators using neighboring points.

1.2.2 Spectral method

Spectral method is generally used when the function is periodic. It gives much better approximation of solution (which is periodic) than any other method. In this method we find the solution of PDEs in Fourier space. Order of convergence in spectral method is O (e−cN) where c is constant and N is number of nodal points. In this method we have to use Discrete Fourier Transform to project the equation in Fourier space and Inverse Discrete Fourier Transform to project back to physical space.

1.2.3 Wavelet Galerkin method

The Galerkin method defines an approximate solution to the weak form of the boundary value problems (BVPs) by restricting the problem to a finite-dimensional subspace. This has the effect of reducing the infinitely many equations to a finite system of equations. Notice that the equation has remained unchanged and only the space have changed. In the past two decades interest in wavelets has been nothing short of remarkable. Wavelets are used in many fields as matrix

compression and approximation theory. In the solution of differential equations, however wavelets have not, thus far, been able to replace other more traditional technique i.e. finite element methods. If we use wavelet basis [15] in place of basis function then this method becomes Wavelet Galerkin Method (WGM).

1.3 Fourier analysis

Signal analysts already have at their disposal an impressive arsenal of tools. Perhaps the most well-known of these is Fourier analysis, which breaks down a signal in to constituent sinusoids of different frequencies. Another way to think of Fourier analysis is as a mathematical technique for transforming our view of the signal from a time-based one to a frequency-based one.

FIGURE 1 Fourier analysis

For many signals, Fourier analysis is extremely useful because the signal's frequency content is of great importance. Fourier analysis has a serious drawback in transforming to the frequency domain where the time information is lost. When looking at a Fourier transform of a signal, it is impossible to tell when a particular event took place.

If a signal doesn't change much over time - that is, if it is what is called a stationary signal- this drawback isn't very important. However, most interesting signals contain numerous non-stationary or transitory characteristics: drift, trends, abrupt changes, and beginnings and ends of

events. These characteristics are often the most important part of the signal, and Fourier analysis is not suited for detecting them.

The heart of spectral finite element method lies in the synthesis of waves using the Fourier transform. A time signal can be represented in the Fourier (frequency) domain in three possible ways, namely the Continuous Fourier Transform (CFT), Fourier series (FS) and Discrete Fourier Transform (DFT). The main advantages of using Fourier transform for structural dynamics and wave propagation problems is that several important characteristics of the system can be directly obtained from the transformed frequency domain. In addition Fourier transforms in principle can achieve high accuracy in differentiation and thus can be used for solution of differential equations.

1.3.1 Continuous Fourier Transforms

The Continuous Fourier Transform pair of a function F(t), defined on the time domain from - ∞ to + ∞, the inverse transform and forward transforms of the time signal can be written as

$$F(t) = \frac{1}{2\pi} \int_{-\infty}^{\infty} \hat{F}(\omega) e^{i\omega t}\, d\omega$$

$$\hat{F}(\omega) = \int_{-\infty}^{\infty} F(t) e^{-i\omega t}\, dt \qquad (1.1)$$

Where $\hat{F}(\omega)$ is the Continuous Fourier Transform (CFT), ω is the angular frequency and i is the complex $\sqrt{-1}$

Example of a rectangular pulse

The application of Fourier transforms, consider a rectangular pulse where the time function is given by

$$F(t) = F_0 \quad -\frac{d}{2} \leq t \leq \frac{d}{2} \qquad \equiv 0 \quad otherwise \tag{1.2}$$

Equation (1.2) substituting in to equation (1.1) gives

$$2\pi\, \hat{F}(\omega) = 2\, F_0 \left\{\frac{\sin(\omega d/2)}{\omega}\right\} \tag{1.3}$$

$$2\pi\, \hat{F}(\omega) = \, F_0 \left\{\frac{\sin(\omega d/2)}{\omega d/2}\right\} \tag{1.4}$$

In this particular case the transform is real-only and symmetric about ω = 0

When the pulse is displaced along the time axis such that the function is given by

$$F(t) = F_0\, t_0 \leq t \, \leq \, t_0 + d \qquad \equiv \, 0 \quad otherwise \tag{1.5}$$

The transform is then

$$2\pi\, \hat{F}(\omega) = \, F_0 d \left\{\left\{\frac{\sin(\omega d/2)}{\omega d/2}\right\}\right\} e^{-i\omega\,(\,t_0 + \frac{d}{2})} \tag{1.6}$$

1.3.2 Discrete Fourier Transform

The Continuous Fourier Transform can only be applied to analytical functions, for example, signals which are given as continuous functions of time. Thus, it cannot be used for numerical analysis. This is a serious limitation as majority of the present day problems are required to be solved numerically. This necessitates a numerical representation of Fourier transform and is termed as Discrete Fourier Transform (DFT). There is however an intermediate form, the Fourier Series (FS), where the inverse transform is written in form of series as

$$F(t) = \frac{1}{2} a_0 + \sum_{n=1}^{\infty} \left[a_n \cos\left(\frac{2\pi n t}{T}\right) + b_n \sin\left(\frac{2\pi n t}{T}\right)\right] \tag{1.7}$$

T is the period of F (t)

It should be noted that the numerical representation of Fourier transform in FS and also in DFT requires a periodicity assumption. The signal is assumed to have a time period T after which it repeats it. The FS coefficients a_n and b_n are obtained from forward transform which is written in integral form

$$a_n = \frac{2}{T}\int_0^T F(t)\cos\left(\frac{2\pi nt}{T}\right)\,dt$$

$$b_n = \frac{2}{T}\int_0^T F(t)\sin\left(\frac{2\pi nt}{T}\right)\,dt \qquad (1.8)$$

n = 0, 1, 2 …

Using the symmetric and anti-symmetric properties of a_n and b_n respectively, equation (1.7) can be rewritten in following exponential form

$$F(t) = \frac{1}{2}\sum_{-\infty}^{\infty}(a_n - ib_n)e^{-i\omega_n t} \qquad (1.9)$$

$$F(t) = \sum_{-\infty}^{\infty}\hat{F}_n e^{i\omega_n t} \qquad (1.10)$$

$$\omega_n = \frac{2\pi n}{T} \qquad (1.11)$$

ω_n= circular frequency

and

$$\hat{F}_n = \frac{1}{2}(a_n - ib_n) = \frac{1}{T}\int_0^T F(t)e^{i\omega_n t}\,dt \qquad (1.12)$$

$$n = 0, \pm 1, \pm 2$$

The main aim of DFT is to replace the integral form of the forward Fourier transform given by equation (1.12) by a summation for numerical implementation.

Let us consider the time signal F(t) is divided in to M equal width rectangles with height F_m which is the value of F(t) at any time instant $t_m, m = 0,1, \ldots\ldots M-1$. The width is the time interval $\Delta t = \frac{T}{M}$. Now knowing that the CFT of a rectangle is a sin function, with the rectangular approximation of the signal, the integral given by the equation (1.12) can be written as the summation of M sin functions of pulse width Δt as follow

$$\hat{F}_n = \Delta t \left[\frac{\sin(\omega_n \frac{\Delta t}{2})}{(\omega_n \frac{\Delta t}{2})}\right] \sum_{m=0}^{M} F_m e^{-i\omega_n t_m} \tag{1.13}$$

For the discretization, Δt is very small which make the value of the sin function given in equation (3.13) nearly equal to unity. Hence the forward and inverse DFT can be written as

$$\hat{F}_n = \hat{F}(\omega_n) = \Delta t \sum_{m=0}^{N-1} F_m e^{-i\omega_n t_m} \tag{1.14}$$

$$= \Delta t \sum_{m=0}^{N-1} F_m e^{-i2\pi nm/N} \tag{1.15}$$

$$F_m = F(t_m) = \frac{1}{T} \sum_{n=0}^{N-1} \hat{F}_n \, e^{i\omega_n t_m} \tag{1.16}$$

$$= \frac{1}{T} \sum_{n=0}^{N-1} \hat{F}_n \, e^{i2\pi nm/N} \tag{1.17}$$

Here, both n and m range from 0 to N-1.

1.3.3 Windowed Fourier transforms

If f (t) is a non-periodic signal, the summation of the periodic functions, sine and cosine, does not accurately represent the signal. We could artificially extend the signal to make it periodic but it would require additional continuity at the end points. The Windowed Fourier Transform (WFT) is one solution to the problem of better representing the non-periodic signal. The WFT can be used to give information about signals simultaneously in the time domain and in the frequency domain. With the WFT, the input signal f(t) is chopped up into sections, and each section is analyzed for its frequency content separately.

1.3.4 Fast Fourier Transforms

To approximate a function by samples, and to approximate the Fourier integral by the Discrete Fourier Transform, requires applying a matrix whose order is the number sample points n. Since multiplying an n x n matrix by a vector costs on the order of n^2 arithmetic operations, the problem gets quickly worse as the number of sample points increases. However, if the samples are uniformly spaced, then the Fourier matrix can be factored in to a product of just a few sparse matrices, and the resulting factors can be applied to a vector in a total of order n log n arithmetic operations. This is the so-called Fast Fourier Transform or FFT.

CHAPTER ~ 2

Literature Review

Graps [21] introduced wavelets to the interested technical person outside of the digital signal processing field. He describes the history of wavelets beginning with Fourier, compares wavelet transforms with Fourier transforms, states properties and other special aspects of wavelets, and finishes with some interesting applications such as image compression, musical tones, and de-noising noisy data.

Latto, Resnikoff and Tanenbaum [35] presented an exact method for evaluating connection coefficients. This is essential for the application of wavelets to the numerical solution of partial differential equations, since numerical approximations of the connection coefficients are in general unstable due to the oscillatory nature of the integrands.

Vonesch, Blu and Unser [68] have presented a novel family of wavelet bases that generalize those introduced by Daubechies*et al.* They are characterized by three essential properties: they are orthonormal (respectively bi-orthogonal), compactly supported and the scaling functions have the ability to reproduce a predefined set of exponential polynomials. The corresponding discrete wavelet transforms have two attractive features. First, their algorithmic implementation is straight forward: it just consists in applying Mallat's fast wavelet transform with scale-dependent filters. Second, the parameters of the exponential polynomials offer new degrees of freedom that have not been explored so far. There is good hope that these can be tuned to the specificities of certain classes of signals. One could envisage applications in several fields, such as speech and audio processing, or neurophysiology. Indeed, these disciplines are concerned with signals that have strong harmonic components or significant exponential trends. Other examples

include the raw time signals encountered in magnetic resonance imaging, RF ultrasound imaging, and optical coherence tomography.

Beylkin [4] describes exact and explicit representations of the differential operators, $\frac{d^n}{dx^n}$, $n = 1, 2, ...$in orthonormal bases of compactly supported wavelets as well as the representations of the Hilbert transform and fractional derivatives. The method of computing these representations is directly applicable to multidimensional convolution operators. Also, sparse representations of shift operators in orthonormal bases of compactly supported wavelets are discussed and a fast algorithm requiring O (N log N) operations for computing the wavelet coefficients of all N circulant shifts of a vector of the length $N = 2^n$ is constructed.

Hariharan [27] considered the beam as partitioned in to several finite elements and the deflection of the beam was required to be a positive quantity along the whole beam so that the related fundamental fourth order ordinary differential equation can continuously holds good. In this paper, he applied Haar wavelet methods to solve finite-length beam differential equations with initial boundary conditions known. An operational matrix of integration based on the Haar wavelet was established and the procedure for applying the matrix to solve the differential equations was formulated. The fundamental idea of Haar wavelet method is to convert the differential equations into a group of algebraic equations, which involves a finite number of variables.

Khatam, et al [33] have presented the harmonic displacement response of a beam utilized as the input signal function in wavelet analysis. In the paper, it was shown that using harmonic

response was superior to the static deflection response and this approach was more effective in the presence of noise and more sensitive to the versatility of the applied harmonic loads.

Williams and Amaratunga [70] have used the wavelet extrapolation method to develop a Discrete Wavelet Transform which was practically free of edge effect. The underlying idea was to use polynomial extrapolation of an order which was typically determined by the number of vanishing moments of wavelets. They described a storage strategy which yields a critically sampled transformed signal at the output of the transformer, and how to obtain perfect reconstruction of the original signal from the transformed signal. The extrapolated Discrete Wavelet Transform was applied to image data and was found to successfully eliminate edge effects in situation where the more conventional circular convolution based Discrete Wavelet Transform produces significant edge effect.

Han,Ren and Huang[26] presented a new spline wavelet finite-element method (FEM). They used the selected spline wavelet scaling functions as the displacement interpolation functions, the finite-element formulations for the typical spline wavelet elements such as plane beam element, in-plane triangular element, in-plane rectangular element, tetrahedral solid element and hexahedral solid elements are derived. It was constructed in a similar way of the conventional displacement based FEM; the proposed spline wavelet finite-element formulations have a wide range of applicability. The numerical examples in structural mechanics has illustrated that the spline wavelet FEM has a high numerical accuracy and fast convergence rate. It was convinced that the wavelet-based methods are powerful in analysing the field problems with changes in gradients and singularities due to the excellent multi-resolution properties of wavelet functions.

Ma et al [44] have constructed a wavelet-based beam element by using Daubechies scaling functions as an interpolating function. Since the nodal lateral displacements and rotations were used as element degrees of freedom, the connection between neighboring elements and boundary conditions has been processed simply as done for traditional elements. Because the transform matrix between wavelet space and physical space was employed to transform elemental DOFs from wavelet coefficients in to lateral displacements and rotations, the compatibility at interfaces between neighboring elements is ensured. So this wavelet-based beam element has been used to analyze the complicated beams such as those with unequal cross section, local load and so on. On the other hand, the boundary conditions have been processed simply as done in traditional elements.

Xiang and Liang [71] presented a method to detect multiple cracks based on frequency information. When a structure was subjected to dynamic or static loads, cracks may develop and the modal frequencies of the cracked structure may change. To detect cracks in a structure, they constructed a high precision wavelet finite element (FE) model of a certain structure using the B-spline wavelet on the interval (BSWI). Cracks have been modeled by rotational springs and added to the FE model. The crack detection database was obtained by solving that model. Then the crack locations and depths were determined based on the frequency information from the database.

Gurley and Kareem [23] worked for the analysis, identification, characterization and simulation of random processes utilizing both the continuous and discrete wavelet transform. The wavelet transform was used to decompose random processes in to localized orthogonal basis functions, providing a convenient format for the modeling, analysis, and simulation of non-stationary

processes. The time and frequency analysis made possible by the wavelet transform provides insight into the character of transient signals through time-frequency maps of the time variant spectral decomposition that traditional approaches miss.

Jameson [28] constructed the wavelet based differentiation matrix for periodic boundary conditions. It has been proved that this matrix displays the very important property of super convergence. The relation between Daubechies-based numerical methods and finite difference methods were explained.

Mitra, Gopalakrishnan and Group [47] presented a wavelet based spectral finite element (WSFE) for studying elastic wave propagation in 1-D connected waveguides. First the partial differential wave equation was converted to simultaneous ordinary differential equations (ODEs) using Daubechies wavelet approximation in time. These ODEs were solved using spectral finite element (SFE) technique by deriving the exact interpolating function in the transformed domain. Spectral element was captured the exact mass distribution and thus the system size required was very much smaller than conventional FE. The localized nature of the compactly supported Daubechies wavelet allowed easy imposition of initial boundary values. This circumvents several disadvantages of the conventional spectral element formulation using Fast Fourier Transforms (FFT) particularly in the study of transient dynamics. The proposed method was used to study longitudinal and flexural wave propagation in rods, beams and frame structures. Numerical experiments are performed to show the advantages over FFT-based spectral element methods. The efficiency of the spectral formulation for impact force identification was also demonstrated.

They extended this WSFE to 2-D wave propagation [49], delamination composite beam [50], axisymmetric cylinder [52], isotropic axisymmetric cylinder [53], Euler-Bernoulli beam with through-width notch type defect [54] and to anisotropic laminated composite plate [55].

Rucka and Wilde [62] presented a method for estimating the damage location in beam and plate structures. A Plexiglass cantilever beam and a steel plate with four fixed boundary conditions were tested experimentally. The estimated mode shapes of the beam were analysed by the one-dimensional continuous wavelet transform. The formulation of the two dimensional continuous wavelet transform for plate damage detection was presented. The location of the damage was indicated by a peak in the spatial variation of the transformed response. Applications of Gaussian wavelet for one-dimensional problems and reverse bi-orthogonal wavelet for two-dimensional structures were presented. The proposed wavelet analysis has effectively identified the defect position without knowledge of neither the structure characteristics nor its mathematical model.

Mitra and Gopalakrishnan [48] have developed a spectrally formulated wavelet finite element which was used not only to study wave propagation in 1-D waveguides but also to extract the wave characteristics, namely the spectrum and dispersion relation for these waveguides. Numerical experiments were performed to study frequency-dependent wave characteristics (dispersion and spectrum relations) in elementary rod, Euler–Bernoulli and Timoshenko beams.

Yaghin and Hesari [72] presented the theory of wavelet analysis including continuous and discrete wavelet transform and applied to Structural Health Monitoring.

Mahmoud and Taha [57] demonstrated that it was possible to establish a damage pattern recognition method by designing a damage classifier that integrates ANN and WMRA. An optimization technique using derivative free optimization (genetic algorithm) was used to identify the optimal ANN architecture. It was shown that the neural-wavelet method established the underlying relationships between the structural dynamic responses (acceleration signals) at the different locations of the structure during healthy performance and that of damaged structure.

Mehra, Patel and Kumar [58] compared three well known methods for solving the PDEs such as Finite Difference Method (FDM), Spectral Method, and Wavelet Galerkin Method (WGM) and tested all these methods on Advection Equation and Klein-Gordon Equation.

Bajaba and Alnefaie [9] presented a new technique that couples modal analysis and wavelet transforms for detection of multiple damages in structures

Sonekar and Mitra [66] presented a wavelet-based method was developed for wave-propagation analysis of a generic multi-coupled one-dimensional periodic structure (PS). The formulation was based on the periodicity condition and uses the dynamic stiffness matrix of the periodic cell obtained from finite-element (FE) or other numerical methods. Here, unlike its conventional definition, the dynamic stiffness matrix was obtained in the wavelet domain through a Daubechies wavelet transform. The proposed numerical scheme enables both time and frequency-domain analysis of PSs under arbitrary loading conditions. This is in contrast to the existing Fourier-transform-based analysis that was restricted to frequency domain study. In this paper, the dispersion characteristics of PSs, especially the band-gap features, are studied. In

addition, the method was implemented to simulate time-domain wave response under impulse loading conditions

Loutridis, Douk and Trochidis [36] presented a method for crack identification in double-cracked beams based on wavelet analysis. The fundamental vibration mode of a double-cracked cantilever beam was analyzed using continuous wavelet transform and both the location and depth of the cracks were estimated. The location of the cracks was determined by the sudden changes in the spatial variation of the transformed response. To estimate the relative depth of the cracks, an intensity factor was established which relates the size of the cracks to the coefficients of the wavelet transform. It was shown that the intensity factor follows definite trends and therefore can be used as an indicator for crack size

Law, Wu and Shi [37] presented a method of moving load and prestress identification using the wavelet-based method in which the approximation of the measured response was used to form the identification equation. This method is for general system identification making use of any types of measured dynamic responses and no assumption is needed on the initial condition of the system.

Kozbial [32] presented a wavelet-based approach for solving two dimensional boundary-value mechanical problems on the example of plate bending. The deflection equation of a bending plate was approximated by two-dimensional Daubechies wavelets using a least-squares Galerkin method. As to the order of the differential equation in mechanics of plate structures was four, a way to perform the calculations of high order connection coefficients (that is, integrals of

products of basis functions with their high order derivatives) was suggested. The implementation of two-dimensional Daubechies scaling functions approximation to plate bending was exhibited numerically.

Lee and Kwon [38] developed a spectral element model for axially moving thin strip-like plates subjected to sudden thermal loadings on their upper or lower surface. First they have derived the governing equations of motion by using the Hamilton's principle and then have formulated the spectral element model from exact wave solutions of the governing equations of motion as the frequency-dependent shape functions by using the variational approach. The extremely high accuracy of the spectral element model has been evaluated by comparing the dynamic responses obtained by the spectral element analysis with those obtained by the conventional finite element analysis. In addition, numerical studies have been conducted to investigate the thermally induced vibrations of a strip-like plate which is axially moving over two simple supports.

Vampa and Diaz [69] showed the feasibility of a hybrid scheme using Daubechies wavelet functions and finite element method to obtain competitive numerical solutions of some classical tests in structural mechanics. Wavelet-based FEM in structural mechanics was proposed by using Daubechies wavelets. The wavelet finite element scheme was constructed in a similar way to the conventional displacement-based FEM: the wavelet functions are used as the displacement interpolation functions and the shape functions were expressed by wavelets. Then, for the Euler Bernoulli beam model, wavelet-finite element formulations were derived.

Zhou and Zhou [73] modified a wavelet approximation for deflections of beams and square thin plates, in which boundary rotational degrees of freedom are included as independent wavelet coefficients. Based on the modified approximations and Hamilton's principle, variation equations for dynamical, statical and buckling problems of square plates are established, without requiring the wavelet approximations or the wavelet basis to satisfy any specific boundary condition in advance. Further, both homogeneous and non-homogeneous boundary conditions, as well as general boundary conditions, of square plates have been treated in the same way as conventional finite element methods. These properties of the method are advantages over current wavelet-Galerkin and wavelet-FEMs.

CHAPTER ~ 3

Wavelet Analysis

3.1 What is wavelet analysis?

A wavelet is a waveform of effectively limited duration that has an average value of zero. Compare wavelets with sine waves, which are the basis of Fourier analysis. Sinusoids do not have limited duration - they extend from minus to plus infinity. And where sinusoids are smooth and predictable, wavelets tend to be irregular and asymmetric.

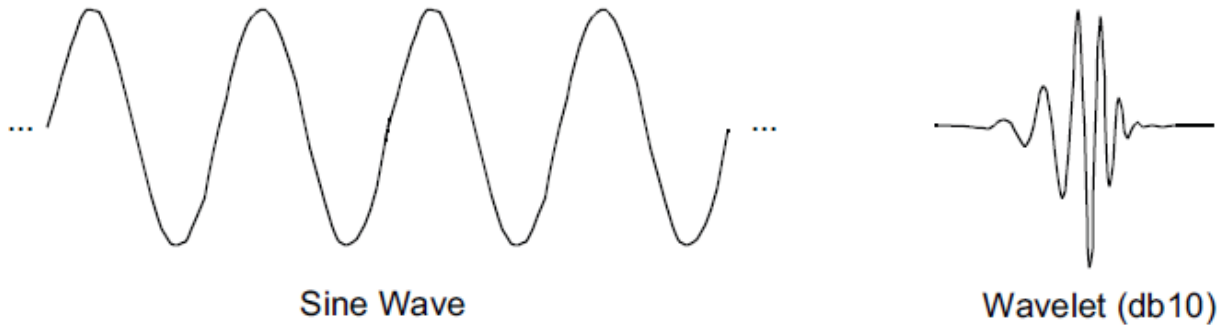

FIGURE 2 wavelet analysis

Fourier analysis consists of breaking up a signal into sine waves of various frequencies. Similarly, wavelet analysis is the breaking up of a signal into shifted and scaled versions of the original (or mother) wavelet. Just looking at figure (2) of wavelets and sine waves, we can see intuitively that signals with sharp changes might be better analyzed with an irregular wavelet than with a smooth sinusoid.

3.2 Definitions of terms used

3.2.1 Orthogonal/Non-orthogonal

Orthogonal wavelet functions will have no overlap with each other (zero correlation) when computing the wavelet transform, while non-orthogonal wavelets will have some overlap (non-zero correlation). Using an orthogonal wavelet, we can transform to wavelet space and back with no loss of information. Non orthogonal wavelet functions tend to artificially add in energy (due

to the overlap) and require renormalization to conserve the information. In general, discrete wavelets are orthogonal while continuous wavelets are non-orthogonal.

3.2.2 Symmetry

It describes the symmetry of the wavelet function about the midpoint. Symmetric Wavelets show no preferred direction in "time," while asymmetric wavelets give unequal Weighting to different directions.

3.2.3 Vanishing Moments

An important property of a wavelet function is the number of vanishing moments, which describes the effect of the wavelet on various signals. A wavelet such as the Daubechies 2 with vanishing moment=2 has zero mean and zero linear trend. When the Daubechies 2 wavelet is used to transform a data series, both the mean and any linear trend are filtered out of the series. A higher vanishing moment implies that more moments (quadratic, cubic, etc.) will be removed from the signal.

3.2.4 Compact Support

This value measures the effective width of the wavelet function. A narrow wavelet function such as the Daubechies order 2 (compact support=3) is fast to compute, but the narrowness in “time" implies a very large width in "frequency." Conversely, wavelets with large compact support such as the Daubechies order 24 (compact support=47) are smoother, have finer frequency resolution and are usually more efficient at de-noising.

3.2.5 Scaling

Scaling a wavelet simply means stretching (or compressing) it. To go beyond colloquial descriptions such as "stretching," introduce the scale factor; often denoted by the letter. If we're talking about sinusoids, for example, the effect of the scale factor is very easy to see.

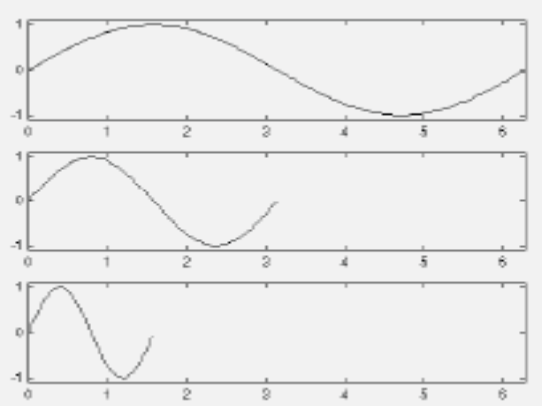

$$f(t) = \sin(t); \quad a = 1$$

$$f(t) = \sin(2t); \quad a = \frac{1}{2}$$

$$f(t) = \sin(4t); \quad a = \frac{1}{4}$$

FIGURE 3 scaling

The scale factor works exactly the same with wavelets. The smaller the scale factor, the more "compressed" the wavelet.

3.2.6 Wavelet $\psi(t)$ and Scaling Functions $\varphi(t)$

The wavelet consists of two components, the scaling function which describes the low-pass filter for the wavelet transform, and the wavelet function which describes the band-pass filter for the transform. Wavelets are defined by the wavelet function $\psi(t)$ (i.e. the mother wavelet) and scaling function $\varphi(t)$ (also called father wavelet) in the time domain. The wavelet function is in effect a band-pass filter and scaling it for each level halves its band width. This creates the problem that in order to cover the entire spectrum, an infinite number of levels would be required. The scaling function filters the lowest of the transform and ensures the entire spectrum is covered.

3.3 Wavelet Transforms:

The word wavelet has been derived from the French world *ondelette* meaning "small wave" and coined by Morletand Grossmann [39, 40, 19]. Some contributors include Morlet and Grossmann [19] for formulation of continuous wavelet transform (CWT), Stromberg [64] for discrete wavelet transform (DWT), Meyer [43] and Mallat [42] for multi-resolution analysis using wavelet transform and Daubechies [15] for orthogonal compactly supported wavelets.

3.3.1 Daubechies Wavelet (db)

Named after Ingrid Daubechies, wavelet transform [15] is defined as a tool that cuts up data or functions or operators in to different frequency components, and then studies each component with a resolution matched to its scale. The Daubechies wavelets are a family of orthogonal wavelets defining a discrete wavelet transform and characterized by a maximal number of vanishing moments for some given support. With each wavelet type of this class, there is a scaling function (also called father wavelet) which generates an orthogonal multi-resolution analysis. In the analysis of time signal, the wavelet transform will decompose the signal in to frequency components and for each of these frequency components.

The forward continuous wavelet transform (CWT) of the F (t) is written as,

$$F^{W}(a,b) = \int_{-\infty}^{\infty} F(t)\ \psi\left(\frac{t-b}{a}\right) \tag{3.1}$$

Here, $\psi(t)$ is the wavelet basis function.

3.3.2 Multi-Resolution Analysis (MRA) with Wavelets

For multi-resolution representation of a function in $L^2(\mathbb{R})$, the mathematical basis of multi-resolution analysis with wavelets, we need to obtain a sequence of closed subspaces V_j for $j \in \mathbb{Z}$ with the following properties,

1. $V_j \subset V_{J+1} \; \forall \; \mathbb{Z}, i.e.,$

$\{0\} \subset V_{-1} \subset V_0 \subset V_1 \subset V_2 \ldots \subset L^2(\mathbb{R})$

2. $\bigcup_{j\in\mathbb{Z}} V_j \; is\; dense\; in\; L^2(\mathbb{R})$

3. $\bigcap_{j\in\mathbb{Z}} V_j = \{0\}$

4. The subspaces are related by a scaling relation,

$F(t) \in V_J \Leftrightarrow F(2t) \in V_{j+1} \qquad \forall \; j \in \mathbb{Z}$

This can also be written as

$$F(t) \in V_j \Leftrightarrow F(2^k t) \in V_{j+k} \; and \; F(t) \in V_J \Leftrightarrow F\left(2^{-j} t\right) \in V_0 \qquad \forall \quad j \in \mathbb{Z}$$

Thus the problem of finding the embedded subspace V_J essentially reduces to the problem of obtaining V_0.

5. Each subspace is spanned by integer translates of a single function,

$$F(t) \in V_j \Leftrightarrow F(t+1) \in V_j \forall \quad j \in \mathbb{Z}$$

From the above properties of MRA it can be concluded that we need to find a scaling function $\varphi(t) \in V_0$ such that its integer translates $\{\varphi(t-k), k \in \mathbb{Z}\}$ are the Riesz bases for the space V_0. Now $\varphi\,(t-k)$ will form a basis for the space V_1. Thus,

$$V_0 = span\left\{\overline{\varphi(t-k), k \in \mathbb{Z}}\right\}$$

$$V_1 = span\left\{\overline{\varphi(2t-k), k \in \mathbb{Z}}\right\}$$

Since $V_0 \in V_1$, the basis functions of space V_0 can be expressed in terms of the basis functions in V_1 as

$$\varphi(t) = \sum_{-\infty}^{\infty} a_k\, \varphi(2t-k) \qquad (3.2)$$

Equation (3.2) is referred to as dilation or scaling relation and $a_k,\ k \in \mathbb{Z}$ are referred to as filter coefficients. The above equation can be solved to derive the scaling function $\varphi(t)$ which forms the bases for space V_0. The basis function for V_j can thus be defined as

$$\varphi_{j,k} = 2^{\frac{j}{2}}\varphi\left(2^j t - k\right) \qquad (3.3)$$

Here, j and k are the dilation and translation indices. In analysis of time signals, j corresponds to the frequency and k to the time.

Let us denote the approximation of the function F (t) by the scaling functions $\varphi_{j,k}(t)$ as $P_j F$. In other words, it is the projection of F (t) in to the subspace V_j,

$$P_j F = \sum_{-\infty}^{\infty} c_{j,k}\varphi_{j,k}(t) \qquad (3.4)$$

Here, $c_{j,k}$ are the approximation coefficients and as $j \to \infty, P_j F \to F$.

The next step is to obtain a closure subspace W_j, $j \in \mathbb{Z}$ for the subspaces V_j and its orthogonal complement such that

$$V_{j+1} = V_j \oplus W_j \ \ and \ \ V_j \perp W_j \tag{3.5}$$

Here, $\oplus$ denotes the direct sum. The subspaces W_j are orthogonal and also

$$\oplus_{j \in \mathbb{Z}} W_j = L^2(\mathbb{R}) \tag{3.6}$$

The wavelet function $\psi(t)$ is defined such that it translates $\psi(t-k)$, $k \in \mathbb{Z}$ are the Riesz bases for W_0. Thus,

$$\psi_{j,k} = 2^{\frac{j}{2}} \psi\left(2^j t - k\right) \tag{3.7}$$

Form the Riesz basis for the subspace W_j. Similar to scaling function $\varphi(t)$ for subspace V_0, the wavelet function $\psi(t)$ for the subspace W_0 can be written as a linear combination of the basis functions for V_1 as $W_0 \subset V_1$,

$$\psi(t) = \sum_{-\infty}^{\infty} b_k \varphi(2t - k) \tag{3.8}$$

Let us consider $Q_J F$ as the approximation of F (t) using wavelet functions $\psi_{j,k}(t)$ and it is the projection of F (t) on the subspace W_j. This can be written as,

$$Q_j F = \sum_{-\infty}^{\infty} d_{j,k} \psi_{j,k}(t) \tag{3.9}$$

Here, $d_{j,k}$ are referred as detail coefficients. Now, using equation (3.5) $P_{j+1}F$ can be written as

$$P_{j+1}F = P_jF + Q_jF \tag{3.10}$$

Thus, the approximation of F(t) at the higher or refined scale is obtained from the approximations at the lower scale with lower resolution. This forms the basis of multi-resolution analysis using wavelets.

3.3.3 Daubechies compactly supported wavelets

It can be summarized from the previous subsection that wavelets $\psi_{j,k}$ form the basis functions for $L^2(\mathbb{R})$ and any function in $L^2(\mathbb{R})$ can be represented using these bases. Several wavelet functions are Morlet wavelets, Shanon wavelets, Meyer wavelets, Mexican hat wavelets have been proposed by the researchers. The choice of wavelet depends on the nature of analysis to be performed. Daubechies [13, 15] proposed orthogonal compactly supported wavelets referred to as Daubechies wavelet. There are other compactly supported wavelets like bi-orthogonal spline (B-spline) wavelets [11, 12], and interpolation wavelets [5, 14].

3.3.4 Construction of Daubechies Compactly Supported Wavelets

The first step in the derivation of these wavelets is to obtain the scaling function $\varphi(t)$ from the scaling or dilation equation given by equation (3.1). The filter coefficients (a_k) determine the nature of the wavelet function and for Deaubechies compactly supported wavelets where only a finite number of filter coefficients are non-zero. $\psi(t)$ is again obtained from $\varphi(t)$ using equation (3.8) and for Daubechies wavelets it can be written as,

$$\psi(t) = \sum_{-\infty}^{\infty} (-1)^k a_{1-k}\, \varphi(2t - k) \tag{3.11}$$

$a_k \ and \ (-1)^k a_k$ form the quadrature mirror filters. The above equation satisfies the orthogonal condition of scaling and wavelet functions required by the equation (3.5). The filter coefficients are obtained by imposing the following constraints on the scaling functions,

1. For uniqueness, normalization is done by considering the area under the scaling function to be unity,

$$\int_{-\infty}^{\infty} \varphi(t)\, dt = 1 \tag{3.12}$$

The above equation leads to the following condition on the filter coefficients,

$$\sum_{-\infty}^{\infty} a_k = 2 \tag{3.13}$$

2. For Daubechies wavelets, the integer translates of scaling functions are orthogonal, i.e.,

$$\int_{-\infty}^{\infty} \varphi(t)\varphi(t+1)dt = \delta_{0,l}\, l \in Z \tag{3.14}$$

where

$$\delta_{0,l} = \begin{cases} 1, & l = 0 \\ 0, & otherwise \end{cases}$$

This gives the condition on the filer coefficients as

$$\sum_{k=-\infty}^{\infty} a_k a_{k+2l} = 2\delta_{0,l}, \quad l \in Z \tag{3.15}$$

3. The condition on the filter coefficients given by equation (3.13) and (3.15) do not given an unique set of filter coefficients. For an N coefficients system, the equation (3.13) and (3.15) provide only $\frac{N}{2} - 1$ equations required to obtain a unique set of filter coefficients we need some other conditions to be imposed on the wavelet functions. For Daubechies wavelets, the conditions are exactly represent polynomial of order M and M = N / 2. Let us consider a polynomial of order M as

$$f(t) = a_0 + a_1 t + a_2 t^2 + \cdots + a_{M-1} t^{M-1} \tag{3.16}$$

The above polynomial should be exactly represent by an expansion similar to that given by equation (3.3) for j = 0 and can be written as

$$f(t) = \sum_{-\infty}^{\infty} c_k \varphi(t-k) \tag{3.17}$$

Since $\psi(t)$are orthogonal to the translates of $\varphi(t)$, taking inner product of equation (3.18) with $\psi(t)$gives

$$\langle f(t), \psi(t) \rangle = \sum_{k=-\infty}^{\infty} c_k \langle \varphi(t-k), \psi(t) \rangle \equiv 0 \tag{3.18}$$

Substituting equation (3.16) in the above equation (3.18) we get

$$\int_{-\infty}^{\infty} \psi(t)\, dt + a_1 \int_{-\infty}^{\infty} \psi(t)\, t\, dt + \cdots + a_{M-1} \int_{-\infty}^{\infty} \psi(t)\, t^M dt \equiv 0 \tag{3.19}$$

The above identity is valid for all $a_j \; for \; j = 0, 1, 2, \ldots M-1$. Choosing $a_l = 1$ and all other $a_j = 0$ gives,

$$\int_{-\infty}^{\infty} \psi(t)\, t^l dt \qquad l = 0, 1, 2, \ldots . M-1 \tag{3.20}$$

This implies that the first M moments of the wavelet function should be zero. Equation (3.20) can be written in terms of the filter coefficients after some calculation as

$$\sum_{-\infty}^{\infty} (-1)^k a_k \, k^l = 0 \;\; l = 0, 1, 2, \ldots, M-1 \tag{3.21}$$

N = 2M determines the order of the Daudechies wavelet and is referred as D4, D6, D8 and thereafter for N = 4, 6, 8 respectively.

As said before, the scaling functions are obtained by solving recursively the dilation equation (3.2) which can be expanded for DN as,

$$\varphi(t) = a_0\varphi(2t) + a_1\varphi(2t-1) + \cdots + a_{N-1}\varphi(2t-N+1) \tag{3.22}$$

Using the compactness criteria of the Daubechies scaling functions between 0 to N – 1 where N is the order of the DN Daubechies scaling function, the relation given in equation (3.22) can be written as the following equations,

$\varphi(0) = a_0\varphi(0)$

$\varphi(1) = a_0\varphi(2) + a_1\varphi(1) + a_2\varphi(0)$

$\varphi(2) = a_0\varphi(4) + a_1\varphi(3) + a_2\varphi(2) + a_3\varphi(1) + a_4\varphi(0)$

$\vdots$

$\varphi(N-2) = a_{N-3}\varphi(N-1) + a_{N-2}\varphi(N-2) + a_{N-1}\varphi(N-3)$

$\varphi(N-1) = a_{N-1}\varphi(N-1)$

This can also be written as matrix form,

$$\begin{bmatrix} a_0 & 0 & 0 & \cdots & 0 & 0 & 0 \\ a_2 & a_1 & a_0 & \cdots & 0 & 0 & 0 \\ a_4 & a_3 & a_2 & \cdots & 0 & 0 & 0 \\ \cdots & \cdots & \cdots & \cdots & \cdots & \cdots & \cdots \\ 0 & 0 & 0 & \cdots & a_{N-3} & a_{N-4} & a_{N-5} \\ 0 & 0 & 0 & \cdots & a_{N-1} & a_{N-2} & a_{N-3} \\ 0 & 0 & 0 & \cdots & 0 & 0 & a_{N-1} \end{bmatrix} \begin{bmatrix} \varphi(0) \\ \varphi(1) \\ \varphi(2) \\ \cdots \\ \varphi(N-3) \\ \varphi(N-2) \\ \varphi(N-1) \end{bmatrix} = \begin{bmatrix} \varphi(0) \\ \varphi(1) \\ \varphi(2) \\ \cdots \\ \varphi(N-3) \\ \varphi(N-2) \\ \varphi(N-1) \end{bmatrix} \quad (3.23)$$

$$B\,\varphi = \varphi$$

Equation (3.23) possesses eigenvalue problems and can be solved to obtain scaling functions $\varphi(t)$ as the eigenvectors. The matrix B is known as the filter coefficients (a_k) and can be solved from equations (3.13), (3.15) and (3.21). The filter coefficients can be obtained using the MATLAB wavelet toolbox function *dfwavf*. The filter coefficients for D4, D6, D12 and D22 are show in table 1.

Once the value of scaling functions $\varphi(t)$ are obtained at the integer values of t between 0 to N-1, the values at the points in between the integers can be obtained from the equation (3.2) modified as

$$\varphi(t/2) = \sum_{-\infty}^{\infty} a_k\, \varphi(t-k) \quad (3.24)$$

These iterations can be done as many times as required to obtain $\varphi(t)$ over a grid of dyadic points. A unique set of φ can be obtained through normalization using equation (3.12).The scaling functions and wavelet functions for Daubechies D4, D6, D12 and D22 with different vanishing moments are shown in figure (4) and figure (5).

TABLE 1:Filter coefficients a_k for Daubechies scaling function with N = 4, 6, 12, 22

k	D4	D6	D12	D22
0	0.6830	0.4705	0.1577	0.0264
1	1.1830	1.1411	0.6995	0.2037
2	0.3170	0.6504	1.0623	0.6363
3	-0.1830	-0.1909	0.4458	0.9697
4		-0.1208	-0.3200	0.5826
5		0.0498	-0.1835	-0.2295
6			0.1379	-0.3878
7			0.0389	0.0934
8			-0.0447	0.2119
9			0.0008	-0.0657
10			0.0068	-0.0940
11			-0.0015	0.0443
12				0.0295
13				-0.0217
14				-0.0047
15				0.0070
16				-0.0004
17				-0.0013
18				0.0004
19				0.0001
20				-0.0000
21				0.0000

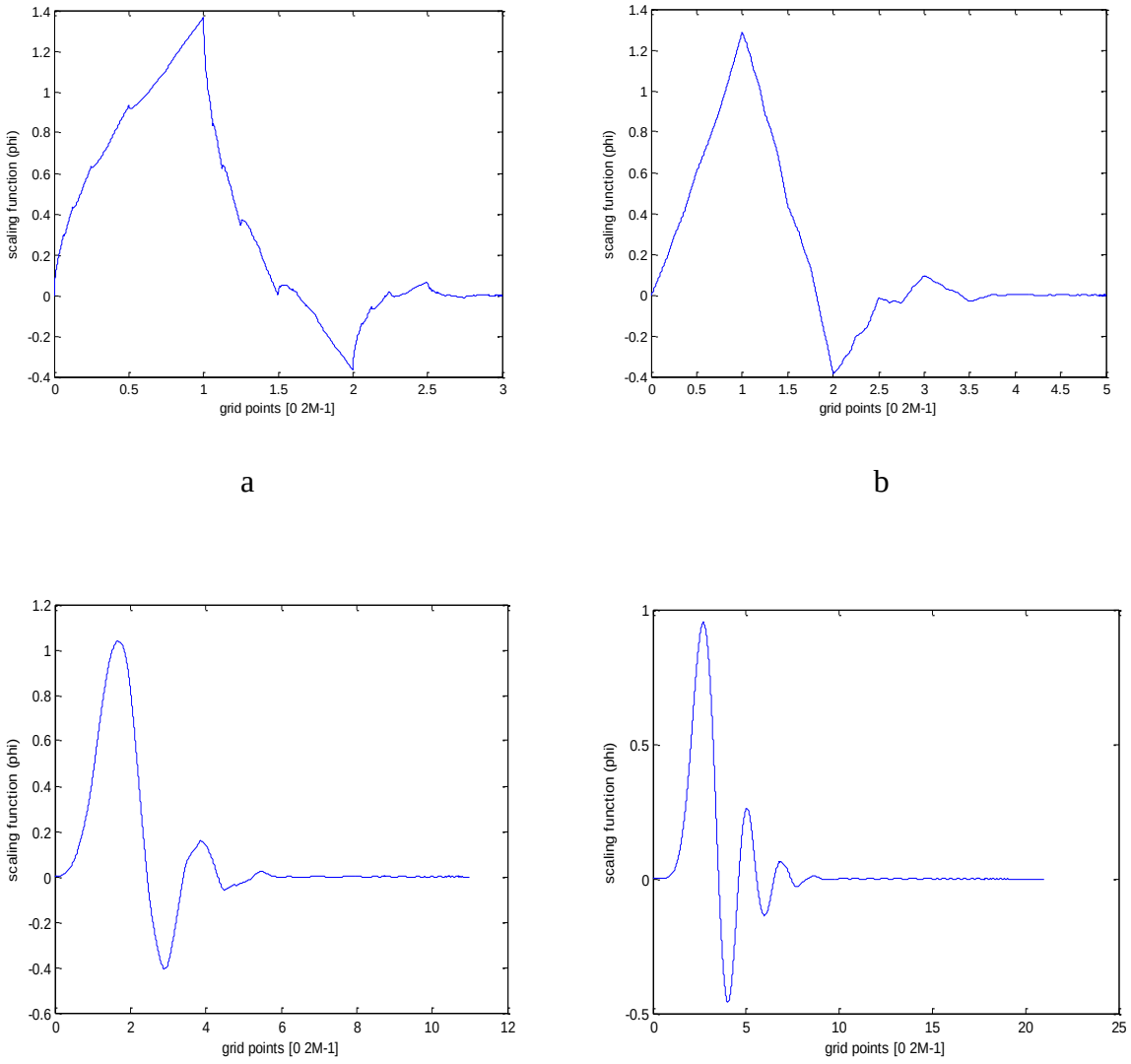

FIGURE 4: Daubechies scaling functions with a) Two vanishing moments. b) Three vanishing moments. c) Six vanishing moments. d) Eleven vanishing moments.

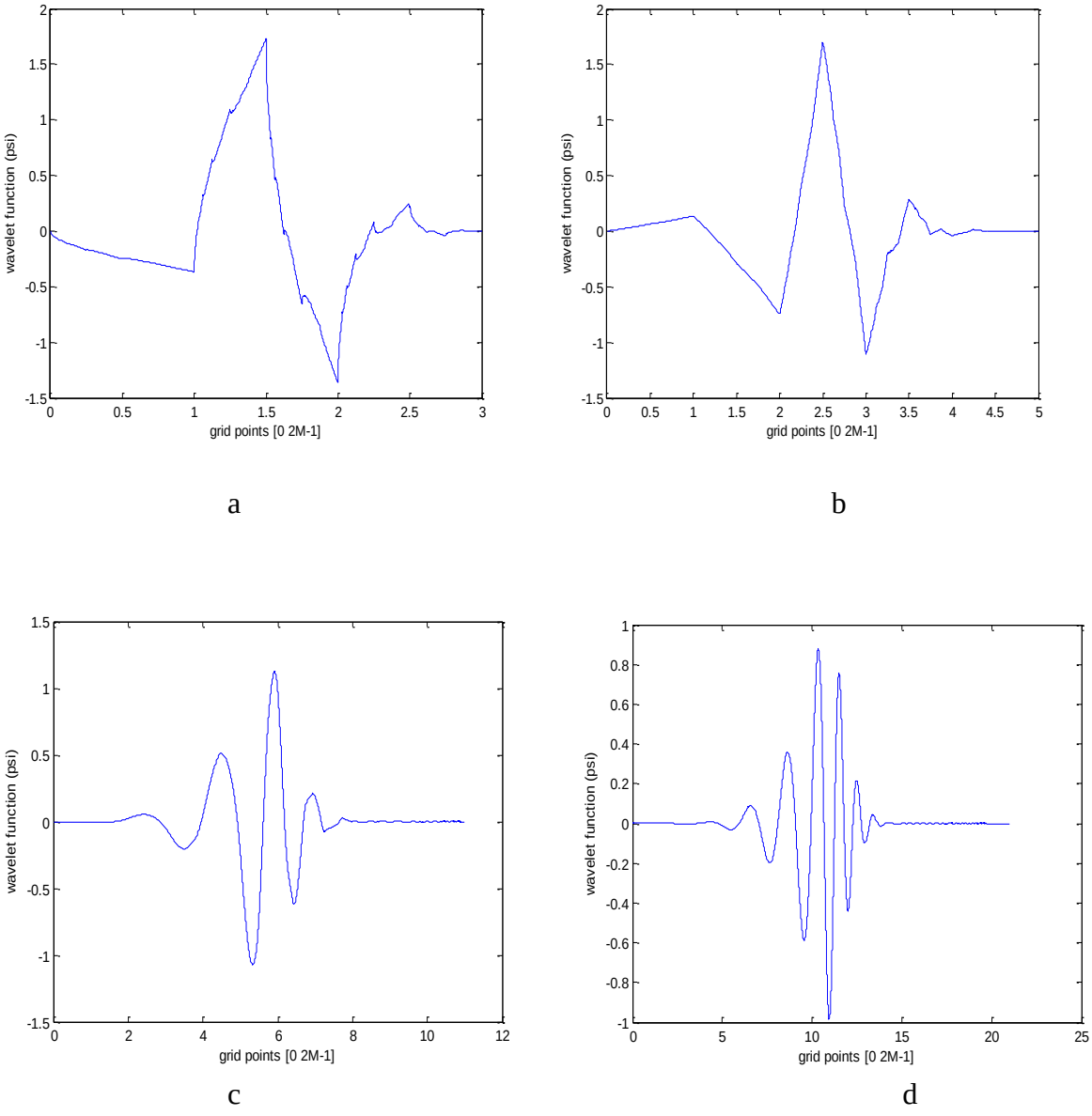

FIGURE 5: Daubechies wavelet functions with a) two vanishing moments. b) Three vanishing moments. c) Six vanishing moments. d) Eleven vanishing moments.

3.4 Moment of Scaling Functions (μ_i^j)

The moment of scaling functions are useful to find the connection coefficients matrix and derived by solving a recursive equation [35]

$$\mu_i^j = \int_{-\infty}^{\infty} x^j \, \varphi(x-i)dx \tag{3.25}$$

$$\mu_0^0 = \int_{-\infty}^{\infty} \varphi(x)dx = 1 \tag{3.26}$$

$$\mu_0^j = \frac{1}{2(2^j-1)} \sum_{k=0}^{j-1} \binom{j}{k} \mu_0^k \left(\sum_{i=0}^{N-1} a_i \, i^{j-k} \right) \tag{3.27}$$

Now that the jth moment of $\varphi(x)$, μ_0^j, has been determined, the moments μ_i^j of the translates of $\varphi(x)$, can be obtained using the formula

$$\mu_i^j = \sum_{k=0}^{j} \binom{j}{k} i^{j-k} \mu_0^k \tag{3.28}$$

The calculated values of moment of scaling functions are shown in table 2 for D6.

TABLE 2: The moment of the scaling functions μ_i^j for D6

S.NO	μ_i^j	
1	μ_0^0	1.0000
2	μ_0^1	0.8174
3	μ_0^2	0.6681
4	μ_1^0	1.0000
5	μ_1^1	1.8174
6	μ_1^2	3.3029
7	μ_2^0	1.0000
8	μ_2^1	2.8174
9	μ_2^2	7.9377
10	μ_3^0	1.0000
11	μ_3^1	3.8174
12	μ_3^2	14.5276
13	μ_4^0	1.0000
14	μ_4^1	4.8174
15	μ_4^2	23.2074

CHAPTER ~ 4

Spectral Analysis

In the spectral analysis wavelet transforms are used to solve wave propagation problems. Spectral analysis helps to study the frequency dependent wave characteristics and finally formulation of Spectral Finite Element Method (SFEM). Spectral Finite Element Method uses spectral analysis to obtain the local wave behavior for different waveguides and hence the wave characteristics, namely the Spectrum and the Dispersion relation. These local characteristics are synthesized to get the global wave behavior. Spectral analysis uses the concepts of Fourier transform, mostly discrete Fourier transform (DFT) are widely used to represent a field variable (say displacement) as a finite series involving a set of coefficients, which requires to be determined based on the boundary conditions of the problems. Spectral analysis enables the determination of two important wave parameters, namely the wavenumbers and the group speeds. These parameters are not only required for spectral element formulation, but also to understand the wave mechanics in a given wave guide. These parameters enable us to know whether the wave mode is a propagating mode or a damping mode or a combination of these two (propagation as well as wave amplitude attenuation). If the wave is propagating, the wavenumber expression will let us know whether it is non-dispersive (i.e. the wave retains its shape as it propagates) or dispersive (i.e. the wave changes its shape as it propagates).

4.1 Spectrum and Dispersion relations

Here, the two important frequency dependent wave characteristics which are spectrum and dispersion relations are obtained for a generalized system using Discrete Fourier Transform. These relations are the frequency variation of the wave parameters termed as wavenumbers and wave speeds respectively. Here, these parameters are explained using the example of a one-dimensional second and fourth order partial differential.First considering the second order partial differential given as,

$$a\frac{\partial^2 u}{\partial x^2} + b\frac{\partial u}{\partial x} = c\frac{\partial^2 u}{\partial t^2} \tag{4.1}$$

where, a, b, and c are dependent on the properties of the known material constants and $u(x,t)$ is the field variable, x is the spatial variable and t is the temporal variable. First transforming the above pertial differential equation (PDE) to frequency domain using DFT .

$$u(x,t) = \sum_{n}^{N-1} \hat{u}_n\,(x,\omega_n)e^{i\omega_n t} \tag{4.2}$$

Where, ω_n is the circular frequency, N is the total number of frequency points and $\hat{u}$ is the frequency dependent Fourier transform of the field varible.

$$\frac{\partial u}{\partial x} = e^{i\omega_n t}\frac{d\hat{u}_n}{dx} \tag{4.2a}$$

$$\frac{\partial^2 u}{\partial x^2} = e^{i\omega_n t}\frac{d^2\hat{u}_n}{dx^2} \tag{4.2b}$$

$$\frac{\partial u}{\partial t} = i\omega_n \hat{u}_n e^{i\omega_n t} \tag{4.2c}$$

$$\frac{\partial^2 u}{\partial t^2} = i^2\omega_n^2 \hat{u}_n e^{i\omega_n t} \tag{4.2d}$$

Subsituting equations (4.2a), (4.2b), (4.2c) and (4.2d) into equation (4.1).

$$a\frac{d^2\hat{u}_n}{dx^2} + b\frac{d\hat{u}_n}{dx} + c\,\omega_n^2\hat{u}_n = 0 \tag{4.3}$$

$$n = 0, \ldots\ldots, N-1$$

We observed from the above equation (4.3), through DFT the governing PDE is reduced to a set of ordinary differential equation (ODE). Equation (4.3) is a constant co-efficients ODE, which has a solution of the type $\hat{u}_n(x,\omega) = A_n e^{ikx}$, where A_n is some unknown constant and k is called the wavenumber.

$$\frac{d\hat{u}_n}{dx} = ik\,A_n e^{ikx} \tag{4.3a}$$

$$\frac{d^2\hat{u}_n}{dx^2} = -k^2 A_n e^{ikx} \tag{4.3b}$$

Substituting the equations (4.3a) and (4.3b) in equation (4.3).

$$\left(k^2 - \frac{bik}{a} - \frac{c\omega_n^2}{a}\right) A_n = 0 \tag{4.4}$$

The above equation is quadratic in k and has two roots corresponding to the two modes of wave propagation correspond to the incident and reflected waves. If the wavenumbers are real, then the wave modes are called propagating modes and if the wavenumbers are complex, then the wave damps out as it propagates and hence they are called evanescent modes.

$$k_{1,2} = \frac{bi}{2a} \pm \sqrt{\frac{-b^2}{4a^2} + \frac{c\omega_n^2}{a}} \tag{4.5}$$

From the equation (4.5) the wave numbers are determined. The wave behaviour is depending upon the values of a, b and c and also depend on the numerical value of the radical $\sqrt{c\omega_n^2/a - b^2/4a^2}$. For example b = 0, the two wavenumbers are,

$$k_1 = \omega_n \frac{c}{a}, \quad k_2 = -\omega_n \frac{c}{a} \tag{4.6}$$

In the above equation (4.6), the wavenumbers are real and hence they are propagating modes. The wavenumbers are linear functions of frequency ω. Here two important wave parameters are there to determine the wave characterstics, namely the phase speed C_p and group speed C_g.

$$C_p = \text{real}\left(\frac{\omega}{k}\right), \quad C_g = \text{real}\left(\frac{d\omega}{dk}\right) \tag{4.7}$$

From the equation (4.6), the phase speed and group speed are,

$$C_p = C_g = \frac{a}{c} \tag{4.8}$$

We observe from the above equation, the phase speed and group speed are constant and equal. Hence, when wavenumbers vary linearly with frequency ω and phase speed and group speed are

equal and constant, then the wave propagates retains its shape called Non-dispersive waves. If the wavenumbers vary non-linearly with frequency ω and phase speed and group speed are not constant but will be functions of frequency i.e. each frequency components travels with different speed as a result, the wave changes its shape as it propagates are called dispersive waves.

Next considering the equation (4.5) with all the constants nonzero. The wavenumbers no longer varies linearly with the frequency. Hence, it can be expected to have dispersive behavior of the waves and the level of dispersion will depend upon the numerical value of the radical. There can be following three cases

1. $\frac{b^2}{4a^2} > \frac{c\omega_n^2}{a}$
2. $\frac{b^2}{4a^2} < \frac{c\omega_n^2}{a}$
3. $\frac{b^2}{4a^2} = \frac{c\omega_n^2}{a}$

Case 1. $\frac{b^2}{4a^2} > \frac{c\omega_n^2}{a}$, then the radical will be a complex number and hence all the wavenumbers will be complex. Hence, the wave modes are called evanescent or a damping mode.

Case 2. $\frac{b^2}{4a^2} < \frac{c\omega_n^2}{a}$, the value of the radical will be positive and real and hence the wavenumber will have both real and imaginary parts i.e. $k = p + jq$, for this case the phase speed and group speed are,

$$C_p = \frac{\omega_n}{k} = \frac{\omega_n}{\sqrt{c\omega_n^2/a - b^2/4a^2}} \tag{4.9}$$

$$C_g = \frac{d\omega_n}{dk} = \frac{a\sqrt{c\omega_n^2/a - b^2/4a^2}}{c\omega_n} \tag{4.10}$$

In the above equations the phase speed and group speed are not same and hence the nature of wave is dispersive. To get the Non-dispersive wave, subsituting b = 0 in equation (4.10).

Case 3. $\frac{b^2}{4a^2} = \frac{c\omega_n^2}{a}$, If the values of the radical will be zero and hence the wavenumber is purely imaginary indicating that the wave mode is a damping mode. Here, the interesting point is to find the transition frequency at which the propagating mode becomes evanescent or a damping mode. This can be obtained by equating the radical to zero. The frequency of transition is given as,

$$\omega_t = \frac{b}{2\sqrt{ac}} \tag{4.11}$$

Once the wavenumbers are obtained, the solution to the governing wave equation (4.3) in the frequency domain can be written as (for b = 0)

$$\hat{u}_n(x, \omega_n) = A_n e^{-ik_n x} + B_n e^{ik_n x} \tag{4.12}$$

$$k_n = \omega_n \sqrt{\frac{c}{a}} \tag{4.13}$$

where A_n represent the incident wave coefficient and B_n represent the reflected wave coefficient. For SFEM, the solution of the governing equation is the starting point in the frequency domain. It can be seen that how the values of the constants in the governing differential equation play an important role in dictating the type of wave propagation.

Now considering the fourth order partial differential equation as

$$A\frac{\partial^4 w}{\partial x^4} + Bw + C\frac{\partial^2 w}{\partial t^2} = 0 \tag{4.14}$$

Here, w is the field variable and A,B,C are material constants.

Now assuming the spectral form of solution to the field variable given as

$$w(x,t) = \sum_{n=0}^{N} \widehat{w}_n(x, \omega_n)\, e^{i\omega_n t} \tag{4.15}$$

where, ω_n is the circular frequency, N is the total number of frequency points and $\widehat{w}$ is the frequency dependent Fourier transform of the field varible.

$$\frac{\partial w}{\partial x} = e^{i\omega_n t}\frac{d\widehat{w}_n}{dx} \tag{4.15a}$$

$$\frac{\partial^2 w}{\partial x^2} = e^{i\omega_n t}\frac{d^2\widehat{w}_n}{dx^2} \tag{4.15b}$$

$$\frac{\partial w}{\partial t} = i\omega_n \widehat{w}_n e^{i\omega_n t} \tag{4.15c}$$

$$\frac{\partial^2 w}{\partial t^2} = i^2\omega_n^2 \widehat{w}_n e^{i\omega_n t} \tag{4.15d}$$

Subsituting equations (4.15a), (4.15b), (4.15c) and (4.15d) into equation (4.15).

$$A\frac{d^4\widehat{w}_n}{dx^4} - (C\omega_n^2 - B)\widehat{w}_n = 0 \tag{4.16}$$

$$n = 0, \ldots\ldots, N-1$$

We observed from the equation (4.16), through DFT the governing PDE is reduced to a set of ordinary differential equation (ODE). Equation (4.16) is a constant co-efficients ODE, which has a solution of the type $\widehat{w}_n(x,\omega) = P_n e^{ikx}$, where P_n is some unknown constant and k is called the wavenumber.

$$\frac{d\widehat{w}_n}{dx} = ik\, P_n e^{ikx} \tag{4.16a}$$

$$\frac{d^2\widehat{w}_n}{dx^2} = -k^2 P_n e^{ikx} \tag{4.16b}$$

Substituting the equations (4.16a) and (4.16b) in equation (4.16).

$$\left(k^4 - \frac{B}{A} + \frac{C\omega_n^2}{A}\right)P_n = 0 \tag{4.17}$$

$$\beta^4 = \left(\frac{C}{A}\omega_n^2 - \frac{B}{A}\right) \tag{4.18}$$

$$k^4 - \beta^4 = 0 \tag{4.19}$$

The above equation is quadratic in k is a fourth order equation corresponding to the four modes of wave propagation two are for the incident and other two for the reflected waves. Also, the wave type is dependend upon the numerical value of $\frac{C\omega_n^2}{A} - \frac{B}{A}$.

Let assuming $\frac{C\omega_n^2}{A} > \frac{B}{A}$ for this case the solution of equation (4.19) will give the following wavenumbers as,

$$k_1 = \beta, \;\; k_2 = -\beta, \;\; k_3 = i\beta, \;\; k_4 = -i\beta, \tag{4.20}$$

In the equation (4.20), k_1 and k_2 are the propagating modes while k_3 and k_4 are the damping or evanescent modes. From the above equation we conclude that the wavenumbers are non-linear functions of the frequency and the mature of waves are dispersive. Also from the above experssion the phase and group speeds for the propagating modes using equations (4.7) and (4.8) are determined.

Next, considering the case when $\frac{C\omega_n^2}{A} < \frac{B}{A}$. For this case, the characteristic equation and the wavenumbers are given as

$$k^4 + \beta^4 = 0 \tag{4.21}$$

$$k_1 = \left[\frac{1}{\sqrt{2}} + i\frac{1}{\sqrt{2}}\right]\beta\,, \qquad k_2 = -\left[\frac{1}{\sqrt{2}} + i\frac{1}{\sqrt{2}}\right]\beta \tag{4.22}$$

$$k_3 = \left[-\frac{1}{\sqrt{2}} + i\frac{1}{\sqrt{2}}\right]\beta\,, \qquad k_4 = -\left[-\frac{1}{\sqrt{2}} + i\frac{1}{\sqrt{2}}\right]\beta \tag{4.23}$$

We observe from the above equation, that the change of sign of $\frac{C\omega_n^2}{A} - \frac{B}{A}$ has caused completely changed wave behavior. We find that all the wavenumbers have both real and the imaginary parts and hence all the modes are propagating as well as attenuating. Also the initial evanescent mode, after a certain frequency, becomes a propagating mode, giving a completely different

wave behavior. The frequency at which this transition takes place is called the cut-off frequency. The cut-off frequency can be obtained if we equate $\frac{C\omega_n^2}{A} - \frac{B}{A}$ to zero,

$$\omega_{cut-off} = \sqrt{\frac{B}{C}} \tag{4.24}$$

The solution of the fourth-order governing equation in the frequency domain (equation (4.16)) can be written as

$$\widehat{w}_n(x, \omega_n) = A_n e^{-i\beta x} + B_n e^{-\beta x} + C_n e^{i\beta x} + D_n e^{\beta x} \tag{4.25}$$

Here, A_n and B_n are the incident wave coefficients and C_n and D_n are the reflected wave coefficients. These can be determined based on the boundry conditions of the problems.

From the above discussion, the direct output of spectral analysis are the spectrum relation, which is a plot of the wavenumber variation with frequency, and dispersion relations, which is a plot of the speed against frequency. These relations are absolute necessary for the spectral finite element formulation.

4.2 Computations of wavenumbers and wave amplitudes

The wavenumbers are obtained as a function of frequency by solving second and fourth order polynomial equations. The determination of wavenumbers are not so straight forward for structures with higher complexities. For one-dimensional structures problems arises when the governing equation is a set of coupled PDEs. In order to handle to such problems, generalized and computationally implementable methods have been proposed [22] to calculate the wavenumbers and wave amplitudes. The two different methods to solve the problems are based on singular value decomposition (SVD) and polynomial eigenvalue problem (PEP) methods. The methods are explained briefly in the following subsections using the example of a Extended Euler-Bernoulli beam.

The governing differential equations of a Extended Euler-Bernoulli beam are given as

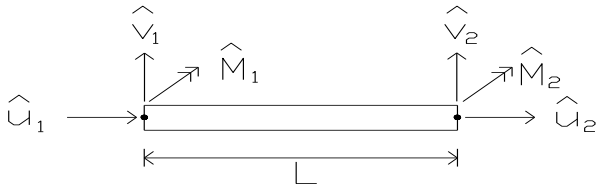

FIGURE 6: Extended Euler-Bernoulli beam

$$\mathrm{EA}\frac{\partial^2 \mathrm{u}}{\partial \mathrm{x}^2} - \eta \mathrm{A}\frac{\partial \mathrm{u}}{\partial \mathrm{t}} = \rho \mathrm{A}\frac{\partial^2 \mathrm{u}}{\partial \mathrm{t}^2} \tag{4.26}$$

$$\mathrm{EI}\frac{\partial^4 \mathrm{w}}{\partial \mathrm{x}^4} + \eta \mathrm{A}\frac{\partial \mathrm{w}}{\partial \mathrm{t}} + \rho \mathrm{A}\frac{\partial^2 \mathrm{w}}{\partial \mathrm{t}^2} = 0 \tag{4.27}$$

The displacements $u(x,t)$ and $w(x,t)$ are transformed to frequency domain using DFT as

$$\mathrm{u}(\mathrm{x},\mathrm{t}) = \sum_{\mathrm{n}=0}^{\mathrm{N}-1} \hat{\mathrm{u}}_\mathrm{n}(\mathrm{x},\omega_\mathrm{n})\, \mathrm{e}^{\mathrm{i}\omega_\mathrm{n}\mathrm{t}} \tag{4.28}$$

$$\mathrm{w}(\mathrm{x},\mathrm{t}) = \sum_{\mathrm{n}=0}^{\mathrm{N}-1} \hat{\mathrm{w}}_\mathrm{n}(\mathrm{x},\omega_\mathrm{n})\, \mathrm{e}^{-\mathrm{i}\omega_\mathrm{n}\mathrm{t}} \tag{4.29}$$

$$\frac{\partial \mathrm{u}}{\partial \mathrm{x}} = \mathrm{e}^{\mathrm{i}\omega_\mathrm{n}\mathrm{t}}\frac{\partial \hat{\mathrm{u}}_\mathrm{n}}{\partial \mathrm{x}} \tag{4.30}$$

$$\frac{\partial^2 \mathrm{u}}{\partial \mathrm{x}^2} = \mathrm{e}^{\mathrm{i}\omega_\mathrm{n}\mathrm{t}}\frac{\partial^2 \hat{\mathrm{u}}_\mathrm{n}}{\partial \mathrm{x}^2} \tag{4.31}$$

$$\frac{\partial \mathrm{u}}{\partial \mathrm{t}} = \mathrm{i}\omega_\mathrm{n}\mathrm{e}^{\mathrm{i}\omega_\mathrm{n}\mathrm{t}}\hat{\mathrm{u}}_\mathrm{n} \tag{4.32}$$

$$\frac{\partial^2 \mathrm{u}}{\partial \mathrm{t}^2} = (\mathrm{i}\omega_\mathrm{n})^2 \mathrm{e}^{\mathrm{i}\omega_\mathrm{n}\mathrm{t}} \hat{\mathrm{u}}_\mathrm{n} = -\omega_\mathrm{n}{}^2 \, \mathrm{e}^{\mathrm{i}\omega_\mathrm{n}\mathrm{t}} \hat{\mathrm{u}}_\mathrm{n} \tag{4.33}$$

$$\frac{\partial \mathrm{w}}{\partial \mathrm{x}} = \mathrm{e}^{\mathrm{i}\omega_\mathrm{n}\mathrm{t}} \frac{\partial \hat{\mathrm{w}}_\mathrm{n}}{\partial \mathrm{x}} \tag{4.34}$$

$$\frac{\partial^4 w}{\partial x^4} = e^{i\omega_n t} \frac{\partial^4 \hat{w}_n}{\partial x^4} \tag{4.35}$$

$$\frac{\partial w}{\partial t} = i\omega_n e^{i\omega_n t} \hat{w}_n \tag{4.36}$$

$$\frac{\partial^2 w}{\partial t^2} = (i\omega_n)^2 e^{i\omega_n t} \hat{w}_n = -\omega_n{}^2 e^{i\omega_n t} \hat{w}_n \tag{4.37}$$

The above equations are substituting into equations (4.26) and (4.27)

$$EA \frac{\partial^2 \hat{u}_n}{\partial x^2} - \eta A i \omega_n \hat{u}_n = -\rho A \omega_n{}^2 \hat{u}_n \tag{4.38}$$

$$EI \frac{\partial^4 \hat{w}_n}{\partial x^4} + \eta A i \omega_n \hat{w}_n - \rho A \omega_n{}^2 \hat{w}_n = 0 \tag{4.39}$$

Assuming the solution of the above equations as

$$\hat{u} = C_u e^{ikx}, \quad \hat{w} = C_w e^{ikx} \tag{4.40}$$

$$-EAk^2 C_u - \eta A i \omega_n C_u = -\rho A \omega_n{}^2 C_u \tag{4.41}$$

$$EAk^2 C_u + \eta A i \omega_n C_u - \rho A \omega_n{}^2 C_u = 0 \tag{4.42}$$

$$EIk^4 C_w + \eta A i \omega_n C_w - \rho A \omega_n{}^2 C_w = 0 \tag{4.43}$$

$$C_u (EAk^2 + \eta A i \omega_n - \rho A \omega_n{}^2) = 0 \tag{4.44}$$

$$C_w(EAk^4 + \eta Ai\omega_n - \rho A{\omega_n}^2) = 0 \tag{4.45}$$

4.2.1 Singular value decomposition (SVD)

In this method the above equations (4.44) and (4.45) are writing in matrix form as

$$\begin{bmatrix} EAk^2 + \eta Ai\omega_n - \rho A{\omega_n}^2 & 0 \\ 0 & EIk^4 + \eta Ai\omega_n - \rho A{\omega_n}^2 \end{bmatrix} \begin{Bmatrix} C_u \\ C_w \end{Bmatrix} \tag{4.46}$$

Here considering damping zero

$$\begin{bmatrix} EAk^4 - \rho A{\omega_n}^2 & 0 \\ 0 & EAk^4 - \rho A{\omega_n}^2 \end{bmatrix} \begin{Bmatrix} C_u \\ C_w \end{Bmatrix} \tag{4.47}$$

$$W(k)\ C\ = 0 \tag{4.48}$$

Here, the k's are the latent roots of the above equation, which satisfy the conditions $\det(W(k)) = 0$ [34]. For each solution of k, there is at least one non-trivial solution for C which is known as the latent eigenvector. To find the latent roots, the determined is expanded in a polynomial of k, p(k), and solved by the companion matrix method. The companion matrix L(p), corresponding to p(k) is formed as

$$L(p) = \begin{bmatrix} 0 & 1 & 0 & \cdots & 0 \\ 0 & 0 & 1 & \cdots & 0 \\ \vdots & \vdots & \vdots & \cdots & \ddots \ \vdots \\ 0 & 0 & \cdots & 0 & 1 \\ -\alpha_m & -\alpha_{m-1} & \cdots & -\alpha_2 & -\alpha_1 \end{bmatrix} \tag{4.49}$$

Where p(k) is given as

$$p(k) = k^m + \propto_1 k^{m-1} + \cdots + \propto_m \tag{4.50}$$

The eigenvalue of $L(p)$ are the roots of $p(k)$, which are obtained using standard techniques. Once the eigenvalues are obtained they are used to obtain the eigenvectors. The eigenvectors are the element of the null space of W (k) and the eigenvalues make this null space non-trivial by rendering W(k) singular. The computation of the eigenvectors is equivalent to computation of the null space of a matrix. For this purpose the SVD method is most effective. U, V and the diagonal matrix S as $A = USV^H$, where H is the Hermitian conjugate. S is the singular value matrix. For singular matrices, one or more of the singular values will be zero and the required property of the unitary matrix V is that the columns of V corresponding to zero singular values are the elements of the null space of A.

4.3 Spectral Finite Element Method (SFEM)

Spectral finite element method is highly suitable for wave propagation analysis as it is in frequency domain. The SFEM in brief is a FE method in the frequency domain which is the main difference between SFEM and FEM.

Finite element method is based on assumed polynomial for displacement. These assumed displacement polynomials are forced to satisfy the weak form of the governing differential equation, which would yield two different matrices namely the stiffness matrix and the mass matrix. These elemental matrices are assembled to obtain the global stiffness and mass matrices. The assemble process ensures equilibrium of forces between the adjacent elements. This procedure will give the discretized form of the governing equation as

$$[M]\{\ddot{u}\} + [C]\{\dot{u}\} + [K]\{u\} = \{F(t)\} \tag{4.26}$$

Where $[M]$ and $[K]$ are the global mass and stiffness matrix and $\{\ddot{u}\}$, $\{\dot{u}\}$ and $\{u\}$ are the acceleration, velocity and displacement vectors.

The above equation is an ODE in time. These equations are solved by the method of mode superposition. As mentioned earlier, the mode superposition method of solution cannot be used for wave propagation analysis. The methods which can be implemented are the time marching schemes [6] which can be either be the explicit or implicit methods. Normally the explicit methods are used for the transient dynamic problem of wave propagation. The solution of the dynamics equation will give displacement, velocity and acceleration histories. The solution time being directly proportional to the number of degree of freedoms, the computational time of such a scheme is very high for wave propagation problems.

On the other hand SFEM uses in most cases the exact solution to the wave equation as its interpolating function. The exact solution will have wave coefficients corresponding to the incident and reflected wave components. If we model for an infinite domain, then the reflected components can be dropped from the interpolating functions are called throw-off elements. This is a great advantage that SFEM have over FEM. Using the interpolation functions for the displacements; the dynamic element stiffness matrix is formulated. The steps involved in the analysis using SFEM are as follows. First the given function is transformed to the frequency domain using the forward FFT. While doing we need to choose the time sampling rate and number of FFT points to decide on the analysis time window. Care should be taken to see that the chosen window is good enough to avoid wraparound problems [16]. The FFT output will yield the frequency, the real and imaginary part of the forcing function, which are stored separately. Over a big frequency loop, the elemental stiffness matrix is generated, assembled and solved as in the case of conventional FEM. The solution process is first performed for a unit impulse, which directly yields the Frequency Response Function (FRF). The FRF is then

convolved with the load to get the required output in the frequency domain. This output is then transformed to the time domain using the inverse FFT.

There are many advantages that SFEM has over conventional FEM. The SFEM can produce results in both the time and frequency domain in a single analysis. Obtaining the FRF is a big advantage of the SFEM. This enables one to solve inverse problems such as the force or the system identification problems.

CHAPTER ~ 5

Wavelet Spectral Finite Element

Wavelet Spectral Finite Element is the development of a wavelet-based numerical technique for simulation of wave propagation in structural waveguides [47]. The method is based on wavelet transform and spectral finite element technique. The orthogonal, compactly supported Daubechies scaling functions are used for temporal approximation followed by finite element approach in the transformed domian. The method termed as Wavelet Spectral Finite Element (WSFE) is ideally suited for modeling finite dimension structures of relatively high complexities. Here, the use of WSFE for modeling one-dimensional waveguide for time domain analysis. The wave propagation analysis is done for an cantilever Extended Euler-Bernoulli aluminum beam with Young's modulus $E = 70 \times 10^9\, N/m^2$ and denity $\rho = 2.7 \times 10^3\, kg/m^3$. The Extended Euler-Bernoulli aluminum beam is fixed at one end and an impulse load shown in figure 7 is applied axial and transvers at the free end. The load is of unit amplitude and duration of 50 μs with a frequency content of 44 KHz. The length, width and depth of Extended Euler-Bernoulli aluminum beam under axail impact load taken as $L = 0.508\, m, b = 0.0254\, m\, and\, d = 0.000254\, m.$ For Extended Euler-Bernoulli aluminum beam under transverse impact load, elastic properties and dimensions are same as the Extended Euler-Bernoulli aluminum beam axial load except the length $L = 0.254\, m.$

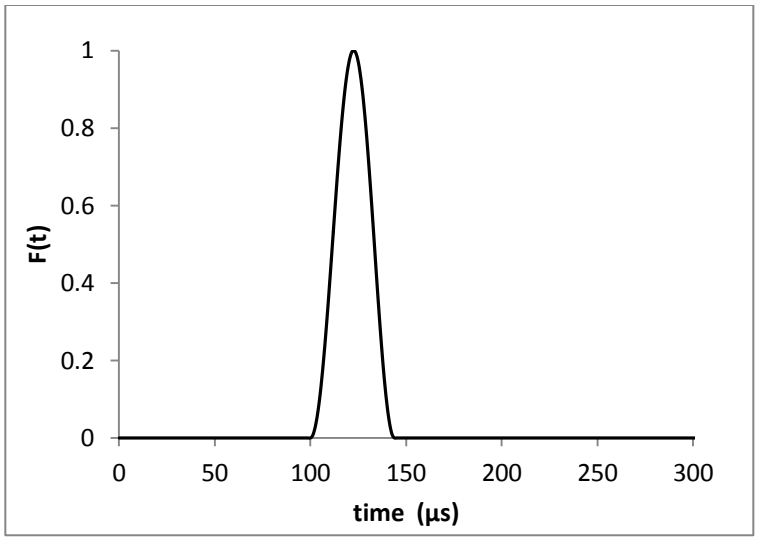

FIGURE 7: Impact load

5.1 Reduction of rod wave equation to ordinary differential equations

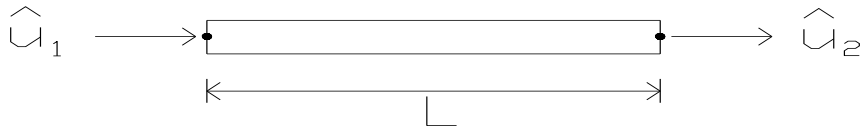

FIGURE 8: Rod element

The governing differential wave equation of an isotropic rod is given as [16]

$$EA\frac{\partial^2 u}{\partial x^2} - \eta A\frac{\partial u}{\partial t} = \rho A\frac{\partial^2 u}{\partial t^2} \tag{5.1}$$

where,

E = Young's modulus

A = cross-sectional area

η = damping ratio

ρ = density of the material

x = spatial coordinates

t = time

$u(x,t)$ = axial displacment

Let $u(x,t)$be discretized at 'n' points in the time window $[0,\ t_f]$. Let $\tau = 0,1,\dots n-1$be the sampling points, then $t_f = (n-1)\Delta t$

$$t = \Delta t\,\tau\,,\ \ \tau = \frac{t}{\Delta t} \tag{5.2}$$

where,

Δt = time interval between two sampling points.

The displacement $u(x,t)$ can be approximated by the scaling function $\varphi(\tau)$ at an arbitrary scale as

$$u(x,t) = u(x,\tau) = \sum_k u_k(x)\,\varphi(\tau - k)\,,\ \ k\ \in \mathbb{Z} \tag{5.3}$$

where,

$u_k(x)$ (Hereafter referred as u_k) is the approximation coefficient at a certain spatial location x. Since now $u(x,t)$ is a function of sum of product of $u_k(x)$ and $\varphi(\tau - k)$ which are uncoupled from the spatial and time variables.

We have;

$$\frac{\partial u}{\partial x} = \sum_k \varphi(\tau - k)\frac{du_k}{dx} \tag{5.3a}$$

$$\frac{\partial^2 u}{\partial x^2} = \sum_k \varphi(\tau - k)\frac{d^2u_k}{dx^2} \tag{5.3b}$$

$$\frac{\partial u}{\partial t} = \sum_k u_k\varphi'(\tau - k)\frac{1}{\Delta t} \tag{5.3c}$$

$$\frac{\partial^2 u}{\partial t^2} = \sum_k u_k \varphi^{"}(\tau - k) \frac{1}{\Delta t^2} \tag{5.3d}$$

Substituting the equations (5.3a), (5.3b), (5.3c) and (5.3d) in equation (5.1) we have the ordinary differential equation (ODE),

$$EA \sum_k \varphi(\tau - k) \frac{d^2 u_k}{dx^2} - \frac{\eta A}{\Delta t} \sum_k u_k \varphi'(\tau - k) = \frac{\rho A}{\Delta t^2} \sum_k u_k \varphi^{"}(\tau - k) \tag{5.4}$$

Taking inner products on both sides of equations (5.4) with $\varphi(\tau - j)$, where, $j = 0,1, \ldots\ldots\ldots, n - 1$, we got,

$$EA \sum_k \frac{d^2 u_k}{dx^2} \int \varphi(\tau - k)\, \varphi(\tau - j) d\tau - \frac{\eta A}{\Delta t} \sum_k u_k \int \varphi'(\tau - k) \varphi(\tau - j)\, d\tau$$

$$= \frac{\rho A}{\Delta t^2} \sum_k u_k \int \varphi^{"}(\tau - k)\, \varphi(\tau - j) d\tau \tag{5.5}$$

Since the translates of scaling functions are orthogonal, we have,

$$\int \varphi(\tau - k)\, \varphi(\tau - j) d\tau = 0 \quad for\ j \neq k \tag{5.6}$$

Equation (5.5) can be written as 'n' simultaneous ODEs by using equation (5.6);

$$EA \frac{d^2 u_j}{dx^2} - \frac{\eta A}{\Delta t} \sum_{k=j-N+2}^{j+N-2} \Omega_{j-k}^1 u_k = \frac{\rho A}{\Delta t^2} \sum_{k=j-N+2}^{j+N-2} \Omega_{j-k}^2 u_k \tag{5.7}$$

where,

$$\Omega_{j-k}^1 = \int \varphi'(\tau - k) \varphi(\tau - j)\, d\tau \tag{5.8}$$

$$\Omega_{j-k}^2 = \int \varphi''(\tau - k) \varphi(\tau - j)\, d\tau \tag{5.9}$$

N = order of the Daubechies wavelet

Ω_{j-k}^1 = first order connection coefficients

Ω_{j-k}^{2}= second order connection coefficients

For compactly supported wavelets, Ω_{j-k}^{1} , Ω_{j-k}^{2} are nonzero only in the interval

$$k = j - N + 2 \; to \; k = j + N - 2.$$

From the equation (5.7);

$$EA\frac{d^2u_j}{dx^2} = \sum_{k=j-N+2}^{j+N+2}\left(\frac{\eta A}{\Delta t}\Omega_{j-k}^{1} + \frac{\rho A}{\Delta t^2}\Omega_{j-k}^{2}\right)u_k \qquad (5.10)$$

The values of the connection coefficients for D22 first and second order are shown in table 3.

TABLE 3: the values of the connection coefficients for first and second order

Ω_1^1	0	Ω_1^2	-3.47337840801057
Ω_2^1	-0.913209538941252	Ω_2^2	2.16026933978281
Ω_3^1	0.347183551085084	Ω_3^2	-0.602653205128255
Ω_4^1	-0.145808621125452	Ω_4^2	0.259980735100996
Ω_5^1	0.0565725329081428	Ω_5^2	-0.113990617900921
Ω_6^1	-0.0189618931390823	Ω_6^2	0.0444431406647273
Ω_7^1	0.00525147114923078	Ω_7^2	-0.0144806539860068
Ω_8^1	-0.00115026373575154	Ω_8^2	0.00377470685481452
Ω_9^1	0.000188643492331173	Ω_9^2	-0.000752954288200255
Ω_{10}^1	-0.0000214714239949848	Ω_{10}^2	0.000108557139788138
Ω_{11}^1	1.56173825099191E-06	Ω_{11}^2	-0.0000103988485588956
Ω_{12}^1	-8.57426004680047E-08	Ω_{12}^2	5.55791376315321E-07
Ω_{13}^1	5.88963918586183E-09	Ω_{13}^2	3.72688117300783E-09
Ω_{14}^1	3.91513557517705E-10	Ω_{14}^2	-5.40977631679387E-09
Ω_{15}^1	-1.13407211122615E-10	Ω_{15}^2	4.73721978304495E-10
Ω_{16}^1	-3.25544726094433E-12	Ω_{16}^2	3.16562432692258E-11
Ω_{17}^1	-1.60928747640703E-14	Ω_{17}^2	2.31293236538858E-13
Ω_{18}^1	-1.06221294110902E-17	Ω_{18}^2	-1.81854918345231E-15
Ω_{19}^1	2.4074144309226E-18	Ω_{19}^2	-1.72101206062974E-16
Ω_{20}^1	1.95845511016976E-17	Ω_{20}^2	1.70753154840549E-16
Ω_{21}^1	-1.16229834607148E-17	Ω_{21}^2	-2.32763511072116E-16

The natural boundary condition associated with the governing differential given by equation (5.1)

$$F = EA\frac{\partial u}{\partial x} \tag{5.11}$$

where, F is the applied axial force and substituting the value from equation (5.3a) in equation (5.11) we have;

$$F = EA\sum_{k}\varphi(\tau - k)\frac{du_k}{dx} \tag{5.12}$$

Taking inner products on both sides of equations (5.12) with $\varphi(\tau - j)$

$$F = EA\sum_{k}\frac{\partial u_k}{\partial x}\int \varphi(\tau - k)\,\varphi(\tau - j) \tag{5.13}$$

Since the translates of scaling functions are orthogonal.

$$F_j = EA\frac{du_j}{dx}\ ,\ \ j = 0,1,\dots,n-1 \tag{5.14}$$

While dealing with finite length data sequence, problems arise at the boundaries. It is observed from the equation (5.10) that certain coefficients u_j near the vicinity of the boundaries ($j = 0\ and\ j = n-1$) lie outside the time window.

5.2 Boundary conditions

The treatment of boundaries for finite domain analysis are dealt as given below. From the equation (5.10) we got n coupled ODEs, which are to be solved for u_j.

5.2.1 Non-perodic boundary conditions

Here the boundaries are treated using wavelet extrapolation method for Daubechies compactly supported wavelets. The formulation details are given in [2, 3, 70]. In this method a polynomial

of order $p-1$, $(p=N/2)$ is assumed to extrapolate the values at the boundaries. Here, the wavelets are used in time, the unknow coefficients on the LHS $(i.e.u_{-1},u_{-2},\dots\dots u_{-N+2})$ are extrapolated from the initial values. The coefficients $u_n,u_{n+1},\dots\dots,u_{n+N-2}$ on RHS are extrapolated from the known coefficients $u_{(n-1)-p+1},u_{(n-1)-p+2},\dots,u_{n-1}$.

Assuming polynomial representation of order $p-1$ for u in the vicinity of $t=0$ and using the equation (5.3)

$$u(x,\tau)=\sum_{k}u_k(x)\,\varphi(\tau-k)=\sum_{l=0}^{p-1}c_l\tau^l \tag{5.15}$$

where c_l are the constant coefficients and using the equation (5.6), taking inner products on both sides of equations (5.15) with $\varphi(\tau-j)$ we have;

$$u_j=\sum_{l=0}^{p-1}c_l\mu_j^l\ ,\quad j=-1,-2,\dots\dots,-N+2 \tag{5.16}$$

where, μ_j^l are the moments of the scaling functions

$$\mu_j^l=\int_{-\infty}^{\infty}\tau^l\,\varphi(\tau-j)d\tau \tag{5.17}$$

The moment of scaling functions are derived in the chapter 3. Solution of equation (5.15) to obtain $c_l$requires $p-1$initial values of $u(x,\tau)\ at\ \tau=0,1,\dots\dots,p-1$. After solving the equation (5.15) we got

$$\begin{Bmatrix}u_0\\u_1\\\vdots\\u_{p-1}\end{Bmatrix}=\begin{bmatrix}0^0 & 0^1 & \cdots & 0^{p-1}\\1^0 & 1^1 & \cdots & 1^{p-1}\\\vdots & \vdots & \cdots & \vdots\\(p-1)^0 & (p-1)^1 & \cdots & (p-1)^{p-1}\end{bmatrix}\begin{Bmatrix}c_1\\c_2\\\vdots\\c_{p-1}\end{Bmatrix} \tag{5.18}$$

$$\begin{Bmatrix} c_1 \\ c_2 \\ \vdots \\ c_{p-1} \end{Bmatrix} = \begin{bmatrix} 0^0 & 0^1 & \cdots & 0^{p-1} \\ 1^0 & 1^1 & \cdots & 1^{p-1} \\ \vdots & \vdots & \cdots & \vdots \\ (p-1)^0 & (p-1)^1 & \cdots & (p-1)^{p-1} \end{bmatrix}^{-1} \begin{Bmatrix} u_0 \\ u_1 \\ \vdots \\ u_{p-1} \end{Bmatrix} \tag{5.19}$$

The values of c_l obtained in terms of the initial values. The unknown coefficient u_j, $j = -1, -2, \ldots\ldots, -N+2$, we have;

$$\begin{bmatrix} u_{-1} \\ u_{-2} \\ \vdots \\ u_{-N+2} \end{bmatrix} = \begin{bmatrix} \mu_{-1}^0 & \mu_{-1}^1 & \cdots & \mu_{-1}^{P-1} \\ \mu_{-2}^0 & \mu_{-2}^1 & \cdots & \mu_{-2}^{P-1} \\ \vdots & \vdots & \cdots & \vdots \\ \mu_{-N+2}^0 & \mu_{-N+2}^1 & \cdots & \mu_{-N+2}^{P-1} \end{bmatrix} \begin{bmatrix} c_0 \\ c_1 \\ \vdots \\ c_{p-1} \end{bmatrix} \tag{5.20}$$

The equation (5.19) subsituting into equation (5.20), we have

$$\begin{bmatrix} u_{-1} \\ u_{-2} \\ \vdots \\ u_{-N+2} \end{bmatrix} = \begin{bmatrix} \mu_{-1}^0 & \mu_{-1}^1 & \cdots & \mu_{-1}^{P-1} \\ \mu_{-2}^0 & \mu_{-2}^1 & \cdots & \mu_{-2}^{P-1} \\ \vdots & \vdots & \cdots & \vdots \\ \mu_{-N+2}^0 & \mu_{-N+2}^1 & \cdots & \mu_{-N+2}^{P-1} \end{bmatrix} \begin{bmatrix} 0^0 & 0^1 & \cdots & 0^{p-1} \\ 1^0 & 1^1 & \cdots & 1^{p-1} \\ \vdots & \vdots & \cdots & \vdots \\ (p-1)^0 & (p-1)^1 & \cdots & (p-1)^{p-1} \end{bmatrix}^{-1} \begin{Bmatrix} u_0 \\ u_1 \\ \vdots \\ u_{p-1} \end{Bmatrix} \tag{5.21}$$

The unknown coefficients at the RHS boundary are determining by assuming same polynomial representation as

$$u_j = \sum_{l=0}^{p-1} c_l u_{j-n}^l \quad j = (n-1) - p + 1, (n-1) - p + 2, \ldots, n-1 \tag{5.22}$$

Equation (5.22) writing matrix form as

$$\begin{bmatrix} u_{(n-1)-p+1} \\ u_{(n-1)-p+2} \\ \vdots \\ u_{(n-1)} \end{bmatrix} = \begin{bmatrix} \mu_{-p}^0 & \mu_{-p}^1 & \cdots & \mu_{-p}^{p-1} \\ \mu_{-p+1}^0 & \mu_{-p+1}^1 & \cdots & \mu_{-p+1}^{p-1} \\ \vdots & \vdots & \cdots & \vdots \\ \mu_{-1}^0 & \mu_{-1}^1 & \cdots & \mu_{-1}^{p-1} \end{bmatrix} \begin{bmatrix} c_0 \\ c_1 \\ \vdots \\ c_{p-1} \end{bmatrix} \tag{5.23}$$

From the above equation (5.23), the c_l values areobtained, we have;

$$\begin{bmatrix} c_0 \\ c_1 \\ \vdots \\ c_{p-1} \end{bmatrix} = \begin{bmatrix} \mu_{-p}^{0} & \mu_{-p}^{1} & \cdots & \mu_{-p}^{p-1} \\ \mu_{-p+1}^{0} & \mu_{-p+1}^{1} & \cdots & \mu_{-p+1}^{p-1} \\ \vdots & \vdots & \cdots & \vdots \\ \mu_{-1}^{0} & \mu_{-1}^{1} & \cdots & \mu_{-1}^{p-1} \end{bmatrix} \begin{bmatrix} u_{(n-1)-p+1} \\ u_{(n-1)-p+2} \\ \vdots \\ u_{(n-1)} \end{bmatrix} \tag{5.24}$$

To get the unknown coefficients at the RHS, subsittiting $j = n, n+1, \ldots\ldots, n-1+N-2$ into equation (5.22), we have;

$$\begin{bmatrix} u_n \\ u_{n+1} \\ \vdots \\ u_{n-1+N-2} \end{bmatrix} = \begin{bmatrix} \mu_{0}^{0} & \mu_{0}^{1} & \cdots & \mu_{0}^{p-1} \\ \mu_{1}^{0} & \mu_{1}^{1} & \cdots & \mu_{1}^{p-1} \\ \vdots & \vdots & \cdots & \vdots \\ \mu_{N-3}^{0} & \mu_{N-3}^{1} & \cdots & \mu_{N-3}^{p-1} \end{bmatrix} \begin{bmatrix} c_0 \\ c_1 \\ \vdots \\ c_{p-1} \end{bmatrix} \tag{5.25}$$

Equation (5.24) substituting into equation (5.25) and finally, these coefficients are substituted into equation (5.10) and the systems of ODEs are written in matrix form, we have;

$$\left\{\frac{d^2 u_j}{dx^2}\right\} = \left(\frac{\eta A}{EA}\Gamma^1 + \frac{\rho A}{EA}\Gamma^2\right)\{u_j\} \tag{5.26}$$

Where, Γ^1 and Γ^2 are the first and second order connection coefficient matrices.

It observed from the above process, the connection coefficient matrices are independent of the problem and depend only on order of the Daubechies wavelet used, i.e. N

5.3 Decoupling using eigenvalue analysis

It can be seen from the above derivations that the wavelet coefficients of first and second derivatives can be obtained as

$$\{\dot{u}_j\} = \Gamma^1\{u_j\} \tag{5.27}$$

$$\{\ddot{u}_j\} = \Gamma^2\{u_j\} \tag{5.28}$$

The second derivative can also be written as

$$\{\ddot{u}_j\} = \Gamma^1\{\dot{u}_j\} \tag{5.29}$$

Substituting equation (5.27) into equation (5.29), we have;

$$\{\ddot{u}_j\} = [\Gamma^1]^2\{u_j\} \tag{5.30}$$

The second order connection coefficient matrix Γ^2 can be determined independently [4], it can be also be written as

$$\Gamma^2 = [\Gamma^1]^2 \tag{5.31}$$

The above modification is done as this helps in imposing the initial conditions for non-perodic solution. Thus the equation (5.26) can be written as

$$\left\{\frac{d^2u_j}{dx^2}\right\} = \left(\frac{\eta A}{EA}\Gamma^1 + \frac{\rho A}{EA}[\Gamma^1]^2\right)\{u_j\} \tag{5.32}$$

In wavelet spectral finite element, the reduced ODEs are coupled, however the system of equation can be decoupled by diagonalizing the connection coefficient matrix. This can be done by eigenvalue analysis of the matrix as

$$\Gamma^1 = \Phi\Pi\Phi^{-1} \tag{5.33}$$

Where Φ is the eigenvector matrix of Γ^1 and Π is the diagonal matrix containing corresponding eigenvalues λ_j. From equation (5.31), Γ^2 can be written as

$$\Gamma^2 = \Phi\Pi^2\Phi^{-1} \tag{5.34}$$

Where Π^2 is a diagonal matrix with diagonal terms λ_j^2. This eigenvalue analysis is costly but can be done once and stored as it is completely independent of the problem.

The ODEs obtained by decoupling the equation (5.32) can be written as

$$\frac{d^2\hat{u}_j}{dx^2} = \left(\frac{\eta A}{EA}\lambda_j + \frac{\rho A}{EA}\lambda_j^2\right)\hat{u}_j \tag{5.35}$$

where,

$$\hat{u}_j = \Phi^{-1}u_j \tag{5.36}$$

Similarly, the forced boundary conditions given in equation (5.14) are similarly transformed as

$$\hat{F}_j = EA\frac{d\hat{u}_j}{dx} \tag{5.37}$$

where,

$$\hat{F}_j = \Phi^{-1}F_j \tag{5.38}$$

5.4 Reduction of beam wave equation to ordinary differential equations

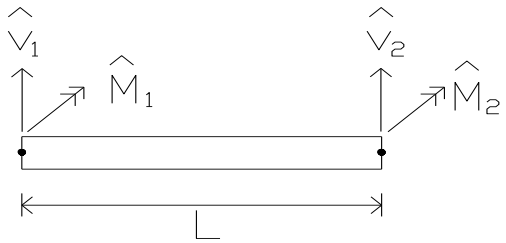

FIGURE 9: Beam element

The flexural wave equation for an Eular-Bernoulli beam has a fourth order derivative in space and is given as [16]

$$EI\frac{\partial^4 w}{\partial x^4} - \eta A\frac{\partial w}{\partial t} + \rho A\frac{\partial^2 w}{\partial t^2} = 0 \tag{5.39}$$

where,

E = Young's modulus

I = moment of inertia

A = cross-sectional area

η = damping ratio

ρ = density of the material

x = spatial coordinates

t = time

$w(x,t)$ = tranverse displacment

Let $w(x,t)$be discretized at 'n' points in the time window $[0,\ t_f]$. Let $\tau = 0,1,\dots n-1$be the sampling points, then $t_f = (n-1)\Delta t$

$$t = \Delta t\,\tau\,,\ \ \tau = \frac{t}{\Delta t} \tag{5.40}$$

where,

Δt = time interval between two sampling points.

The displacement $w(x,t)$ can be approximated by the scaling function $\varphi(\tau)$ at an arbitrary scale as

$$w(x,t) = w(x,\tau) = \sum_k w_k(x)\,\varphi(\tau - k)\,,\ \ k\ \in \mathbb{Z} \tag{5.41}$$

where,

$w_k(x)$(Hereafter referred as w_k) is the approximation coefficient at a certain spatial location x. Since now $w(x,t)$ is a function of sum of product of $w_k(x)$ and $\varphi(\tau - k)$ which are uncoupled from the spatial and time variables

We have;

$$\frac{\partial w}{\partial x} = \sum_k \varphi(\tau - k)\frac{dw_k}{dx} \tag{5.41a}$$

$$\frac{\partial^2 w}{\partial x^2} = \sum_k \varphi(\tau - k)\frac{d^2 w_k}{dx^2} \tag{5.41b}$$

$$\frac{\partial^3 w}{\partial x^3} = \sum_k \varphi(\tau - k)\frac{d^3 w_k}{dx^3} \tag{5.41c}$$

$$\frac{\partial^4 w}{\partial x^4} = \sum_k \varphi(\tau - k)\frac{d^4 w_k}{dx^4} \tag{5.41d}$$

$$\frac{\partial w}{\partial t} = \sum_k w_k \varphi'(\tau - k) \frac{1}{\Delta t} \tag{5.41e}$$

$$\frac{\partial^2 w}{\partial t^2} = \sum_k w_k \varphi^{"}(\tau - k) \frac{1}{\Delta t^2} \tag{5.41f}$$

Substituting the equations (5.41a), (5.41b), (5.41c), (5.41d), (5.41e) and (5.41f) in equation (5.39) we have the ordinary differential equation (ODE),

$$EI \sum_k \varphi(\tau - k) \frac{d^4 w_k}{dx^4} + \frac{\eta A}{\Delta t} \sum_k w_k \varphi'(\tau - k) + \frac{\rho A}{\Delta t^2} \sum_k w_k \varphi^{"}(\tau - k) = 0 \tag{5.42}$$

Taking inner products on both sides of equations (5.42) with $\varphi(\tau - j)$, Where, $j = 0,1, \dots \dots \dots, n-1$, we get,

$$EI \sum_k \frac{d^4 w_k}{dx^4} \int \varphi(\tau - k)\, \varphi(\tau - j) d\tau + \frac{\eta A}{\Delta t} \sum_k w_k \int \varphi'(\tau - k) \varphi(\tau - j)\, d\tau$$

$$+ \frac{\rho A}{\Delta t^2} \sum_k w_k \int \varphi^{"}(\tau - k)\, \varphi(\tau - j) d\tau = 0 \tag{5.43}$$

Since the translates of scaling functions are orthogonal, we have,

$$\int \varphi(\tau - k)\, \varphi(\tau - j) d\tau = 0 \quad for\ j \neq k \tag{5.44}$$

Equation (5.43) can be written as 'n' simultaneous ODEs by using equation (5.44);

$$EI \frac{d^4 w_j}{dx^4} + \frac{\eta A}{\Delta t} \sum_{k=j-N+2}^{j+N-2} \Omega_{j-k}^1 w_k + \frac{\rho A}{\Delta t^2} \sum_{k=j-N+2}^{j+N-2} \Omega_{j-k}^2 w_k = 0 \tag{5.45}$$

where,

$$\Omega_{j-k}^1 = \int \varphi'(\tau - k) \varphi(\tau - j)\, d\tau \tag{5.46}$$

$$\Omega_{j-k}^2 = \int \varphi''(\tau - k) \varphi(\tau - j)\, d\tau \tag{5.47}$$

N = order of the Daubechies wavelet

Ω_{j-k}^{1} = first order connection coefficients

Ω_{j-k}^{2}= second order connection coefficients

For compactly supported wavelets, Ω_{j-k}^{1} , Ω_{j-k}^{2} are nonzero only in the interval

$$k = j - N + 2 \; to \; k = j + N - 2.$$

From the equation (5.45);

$$EI\frac{d^4 w_j}{dx^4} = \sum_{k=j-N+2}^{j+N+2} \left(\frac{\eta A}{\Delta t}\Omega_{j-k}^{1} + \frac{\rho A}{\Delta t^2}\Omega_{j-k}^{2}\right) w_k = 0 \tag{5.48}$$

The natural boundary condition associated with the governing differential given by equation (5.39)

$$\mathrm{M} = \mathrm{EI}\,\frac{\partial^2 w}{\partial x^2} \tag{5.49}$$

$$-\mathrm{V} = \mathrm{EI}\,\frac{\partial^3 w}{\partial x^3} \tag{5.50}$$

Where, M and V are the applied moment and transverse force and substituting the value from equations (5.41b) and (5.41c) in equations (5.49) and (5.50) we have;

$$M = \mathrm{EI}\sum_k \varphi(\tau - k)\frac{d^2 w_k}{dx^2} \tag{5.51}$$

$$-V = EI\sum_k \varphi(\tau - k)\frac{d^3 w_k}{dx^3} \tag{5.52}$$

Taking inner products on both sides of equations (5.51) and (5.52) with $\varphi(\tau - j)$, we have;

$$\mathrm{M} = \mathrm{EI}\sum_k \frac{\partial^2 w_k}{\partial x^2}\int \varphi(\tau - k)\,\varphi(\tau - j) \tag{5.53}$$

$$-\mathrm{V} = \mathrm{EI}\sum_k \frac{\partial^3 w_k}{\partial x^3}\int \varphi(\tau - k)\,\varphi(\tau - j) \tag{5.54}$$

Since the translates of scaling functions are orthogonal.

$$\mathrm{M}_j = \mathrm{EI}\,\frac{d^2 w_j}{dx^2}\,,\quad j = 0,1,\ldots,n-1 \tag{5.55}$$

$$-\mathrm{V}_j = \mathrm{EI}\,\frac{d^3 w_j}{dx^3}\,,\quad j = 0,1,\ldots,n-1 \tag{5.56}$$

While dealing with finite length data sequence, problems arise at the boundaries. It observed from the equation (5.48) that certain coefficients w_j near the vicinity of the boundaries ($j = 0\ and\ j = n-1$) lie outside the time window.

5.5 Boundary conditions

The treatment of boundaries for finite domain analysis. From the equation (5.48) we got n coupled ODEs, which are to be solved for w_j.

5.5.1 Non-perodic boundary conditions

Here the boundaries are treating using wavelet extrapolation method for Daubechies compactly supported wavelets. The formulation details are given in [2, 3, 70]. In this method apolynomial of order $p-1,\ (p = N/2)$ is assumed to extrapolate the values at the boundaries. Here, the wavelets are used in time, the unknow coefficients on the LHS ($i.e.\, w_{-1}, w_{-2}, \ldots\ldots w_{-N+2}$) are extrapolated from the initial values. The coefficients $w_n, w_{n+1}, \ldots\ldots, w_{n+N-2}$ on RHS are extrapolated from the known coefficients $w_{(n-1)-p+1}, w_{(n-1)-p+2}, \ldots, w_{n-1}$.

Assuming polynomial representation of order $p-1$ for u in the vicinity of $t = 0$ and using the equation (5.41)

$$w(x,\tau) = \sum_k w_k(x)\,\varphi(\tau - k) = \sum_{l=0}^{p-1} c_l \tau^l \tag{5.57}$$

Where c_l are the constant coefficients and using the equation (5.44), taking inner products on both sides of equations (5.57) with $\varphi(\tau - j)$ we have;

$$w_j = \sum_{l=0}^{p-1} c_l \mu_j^l \ , \quad j = -1, -2, \ldots, -N+2 \tag{5.58}$$

Where, μ_j^l are the moments of the scaling functions

$$\mu_j^l = \int_{-\infty}^{\infty} \tau^l \, \varphi(\tau - j) d\tau \tag{5.59}$$

The moment of scaling functions are derived in the chapter 3. Solution of equation (5.57) to obtain $c_l$requires $p-1$initial values of $u(x,\tau)\, at\ \tau = 0,1, \ldots, p-1$. After solving the equation (5.57) we got

$$\begin{Bmatrix} w_0 \\ w_1 \\ \vdots \\ w_{p-1} \end{Bmatrix} = \begin{bmatrix} 0^0 & 0^1 & \cdots & 0^{p-1} \\ 1^0 & 1^1 & \cdots & 1^{p-1} \\ \vdots & \vdots & \cdots & \vdots \\ (p-1)^0 & (p-1)^1 & \cdots & (p-1)^{p-1} \end{bmatrix} \begin{Bmatrix} c_0 \\ c_1 \\ \vdots \\ c_{p-1} \end{Bmatrix} \tag{5.60}$$

$$\begin{Bmatrix} c_0 \\ c_1 \\ \vdots \\ c_{p-1} \end{Bmatrix} = \begin{bmatrix} 0^0 & 0^1 & \cdots & 0^{p-1} \\ 1^0 & 1^1 & \cdots & 1^{p-1} \\ \vdots & \vdots & \cdots & \vdots \\ (p-1)^0 & (p-1)^1 & \cdots & (p-1)^{p-1} \end{bmatrix}^{-1} \begin{Bmatrix} w_0 \\ w_1 \\ \vdots \\ w_{p-1} \end{Bmatrix} \tag{5.61}$$

The values of c_l obtained in terms of the initial values. The unknown coefficient u_j , $j = -1, -2, \ldots \ldots, -N+2$, we have;

$$\begin{bmatrix} w_{-1} \\ w_{-2} \\ \vdots \\ w_{-N+2} \end{bmatrix} = \begin{bmatrix} \mu_{-1}^0 & \mu_{-1}^1 & \cdots & \mu_{-1}^{P-1} \\ \mu_{-2}^0 & \mu_{-2}^1 & \cdots & \mu_{-2}^{P-1} \\ \vdots & \vdots & \cdots & \vdots \\ \mu_{-N+2}^0 & \mu_{-N+2}^1 & \cdots & \mu_{-N+2}^{P-1} \end{bmatrix} \begin{bmatrix} c_0 \\ c_1 \\ \vdots \\ c_{p-1} \end{bmatrix} \tag{5.62}$$

The equation (5.19) subsituting into equation (5.20), we have

$$\begin{bmatrix} w_{-1} \\ w_{-2} \\ \vdots \\ w_{-N+2} \end{bmatrix} = \begin{bmatrix} \mu_{-1}^{0} & \mu_{-1}^{1} & \cdots & \mu_{-1}^{P-1} \\ \mu_{-2}^{0} & \mu_{-2}^{1} & \cdots & \mu_{-2}^{P-1} \\ \vdots & \vdots & \cdots & \vdots \\ \mu_{-N+2}^{0} & \mu_{-N+2}^{1} & \cdots & \mu_{-N+2}^{P-1} \end{bmatrix} \begin{bmatrix} 0^0 & 0^1 & \cdots & 0^{p-1} \\ 1^0 & 1^1 & \cdots & 1^{p-1} \\ \vdots & \vdots & \cdots & \vdots \\ (p-1)^0 & (p-1)^1 & \cdots & (p-1)^{p-1} \end{bmatrix}^{-1} \begin{Bmatrix} u_0 \\ u_1 \\ \vdots \\ u_{p-1} \end{Bmatrix} \quad (5.63)$$

The unknown coefficients at the RHS boundary are determining by assuming same polynomial representation as

$$w_j = \sum_{l=0}^{p-1} c_l u_{j-n}^{l} \quad j = (n-1)-p+1, (n-1)-p+2, \dots, n-1 \quad (5.64)$$

Equation (5.64) writing matrix form as

$$\begin{bmatrix} w_{(n-1)-p+1} \\ w_{(n-1)-p+2} \\ \vdots \\ w_{(n-1)} \end{bmatrix} = \begin{bmatrix} \mu_{-p}^{0} & \mu_{-p}^{1} & \cdots & \mu_{-p}^{p-1} \\ \mu_{-p+1}^{0} & \mu_{-p+1}^{1} & \cdots & \mu_{-p+1}^{p-1} \\ \vdots & \vdots & \cdots & \vdots \\ \mu_{-1}^{0} & \mu_{-1}^{1} & \cdots & \mu_{-1}^{p-1} \end{bmatrix} \begin{bmatrix} c_0 \\ c_1 \\ \vdots \\ c_{p-1} \end{bmatrix} \quad (5.65)$$

From the above equation (5.65), the c_l values are obtained, we have;

$$\begin{bmatrix} c_0 \\ c_1 \\ \vdots \\ c_{p-1} \end{bmatrix} = \begin{bmatrix} \mu_{-p}^{0} & \mu_{-p}^{1} & \cdots & \mu_{-p}^{p-1} \\ \mu_{-p+1}^{0} & \mu_{-p+1}^{1} & \cdots & \mu_{-p+1}^{p-1} \\ \vdots & \vdots & \cdots & \vdots \\ \mu_{-1}^{0} & \mu_{-1}^{1} & \cdots & \mu_{-1}^{p-1} \end{bmatrix} \begin{bmatrix} w_{(n-1)-p+1} \\ w_{(n-1)-p+2} \\ \vdots \\ w_{(n-1)} \end{bmatrix} \quad (5.66)$$

To get the unknown coefficients at the RHS, subsittting $j = n, n+1, \dots\dots, n-1+N-2$ into equation (5.64), we have;

$$\begin{bmatrix} w_n \\ w_{n+1} \\ \vdots \\ w_{n-1+N-2} \end{bmatrix} = \begin{bmatrix} \mu_{0}^{0} & \mu_{0}^{1} & \cdots & \mu_{0}^{p-1} \\ \mu_{1}^{0} & \mu_{1}^{1} & \cdots & \mu_{1}^{p-1} \\ \vdots & \vdots & \cdots & \vdots \\ \mu_{N-3}^{0} & \mu_{N-3}^{1} & \cdots & \mu_{N-3}^{p-1} \end{bmatrix} \begin{bmatrix} c_0 \\ c_1 \\ \vdots \\ c_{p-1} \end{bmatrix} \quad (5.67)$$

Equation (5.66) substituting into equation (5.67) and finally, these coefficients are substituted into equation (5.52) and the systems of ODEs are written in matrix form, we have;

$$\left\{\frac{d^4 w_j}{dx^4}\right\} + \left(\frac{\eta A}{EI}\Gamma^1 + \frac{\rho A}{EI}\Gamma^2\right)\{w_j\} = 0 \tag{5.68}$$

Where, Γ^1 and Γ^2 are the first and second order connection coefficient matrices.

It observed from the above process, the connection coefficient matrices are independent of the problem and depend only on order of the Daubechies wavelet used, i.e. N

5.6 Decoupling using eigenvalue analysis

It can be seen from the above derivations that the wavelet coefficients of first and second derivatives can be obtained as

$$\{\dot{w}_j\} = \Gamma^1\{w_j\} \tag{5.69}$$

$$\{\ddot{w}_j\} = \Gamma^2\{\mathrm{w_j}\} \tag{5.70}$$

The second derivative can also be written as

$$\{\ddot{w}_j\} = \Gamma^1\{\dot{\mathrm{w}}_\mathrm{j}\} \tag{5.71}$$

Substituting equation (5.69) into equation (5.71), we have;

$$\{\ddot{w}_j\} = [\Gamma^1]^2\{w_j\} \tag{5.72}$$

The second order connection coefficient matrix Γ^2 can be determined independently [4], it can be also be written as

$$\Gamma^2 = [\Gamma^1]^2 \tag{5.73}$$

The above modification is done as this helps in imposing the initial conditions for non-perodic solution. Thus the equation (5.68) can be written as

$$\left\{\frac{d^4 w_j}{dx^4}\right\} + \left(\frac{\eta A}{EI}\Gamma^1 + \frac{\rho A}{EI}[\Gamma^1]^2\right)\{w_j\} = 0 \tag{5.74}$$

In wavelet spectral finite element, the reduced ODEs are coupled, however the system of equation can be decoupled by diagonalizing the connection coefficient matrix. This can be done by eigenvalue analysis of the matrix as

$$\Gamma^1 = \Phi \Pi \Phi^{-1} \tag{5.75}$$

where Φ is the eigenvector matrix of Γ^1 and Π is the diagonal matrix containing corresponding eigenvalues λ_j. From equation (5.73), Γ^2 can be written as

$$\Gamma^2 = \Phi \Pi^2 \Phi^{-1} \tag{5.76}$$

where Π^2 is a diagonal matrix with diagonal terms λ_j^2. This eigenvalue analysis is costly but can be done once and stored as it is completely independent of the problem.

The ODEs obtained by decoupling the equation (5.74) can be written as

$$\frac{d^4 \widehat{w}_j}{dx^4} + \left(\frac{\eta A}{EI} \lambda_j + \frac{\rho A}{EI} \lambda_j^2 \right) \widehat{w}_j = 0 \tag{5.77}$$

where,

$$\widehat{w}_j = \Phi^{-1} w_j \tag{5.78}$$

Similarly, the forced boundary conditions given in equation (5.56) are similarly transformed as

$$\widehat{\mathrm{M}}_j = \mathrm{EI} \, \frac{d^2 \widehat{w}_j}{dx^2} \tag{5.79}$$

$$-\widehat{V}_j = \mathrm{EI} \, \frac{d^3 \widehat{w}_j}{dx^3} \tag{5.80}$$

CHAPTER ~ 6

Wavelet Spectral Finite Element Formulation

6.1 Spectral element formulation for Extended Eular-Bernoulli beam

The Extended Euler-Bernoulli beam element with two nodes and three degree of freedoms (dof) at each node namely, $\hat{u}$, $\hat{w}$ and $\hat{\theta}$ shown in figure 6. The exact interpolating function obtained by solving equations (5.35) and (5.77) we have;

$$\hat{u}(x) = c_1 e^{-ik_1 x} + c_2 e^{-ik_1(L-x)} \tag{6.1}$$

$$\hat{w}(x) = C_3 e^{-ik_2 x} + C_4 e^{-ik_2(L-x)} + C_5 e^{-ik_3 x} + C_6 e^{-ik_3(L-x)} \tag{6.2}$$

$$\frac{\partial \hat{w}(x)}{\partial x} = \hat{\theta}(x) = -ik_2 C_3 e^{-ik_2 x} + ik_2 C_4 e^{-ik_2(L-x)} - ik_3 C_5 e^{-ik_3 x} + k_3 C_6 e^{-ik_3(L-x)} \tag{6.3}$$

The equations (6.1), (6.2) and (6.3) are writing in matrix form as

$$\begin{Bmatrix} \hat{\mathrm{u}}(\mathrm{x}) \\ \hat{\mathrm{w}}(\mathrm{x}) \\ \hat{\theta}(\mathrm{x}) \end{Bmatrix} = [\mathrm{R}][\theta_D]\{\mathrm{C}\} \tag{6.4}$$

where

k are the wave numbers are obtained from the latent root given in chapter 4.

[Θ]is a diagonal matrix with diagonal terms $\left[e^{-ik_1 x}, e^{-ik_1(L-x)}, e^{-ik_2 x}, e^{-ik_2(L-x)}, e^{-ik_3 x}, e^{-ik_3(L-x)}\right]$

$[R]$is the 3x6 amplitude ratio matrix obtained by solving SVD, in addition to the wave numbers

$[R]$is the eigenvector matrix while the wave numbers are the eigenvalues

$$[R] = \begin{bmatrix} R_{11} & R_{12} & 0 & 0 & 0 & 0 \\ 0 & 0 & R_{21} & R_{22} & R_{23} & R_{24} \\ 0 & 0 & R_{31} & R_{32} & R_{33} & R_{34} \end{bmatrix} \tag{6.5}$$

$\{C\} = \{C_1 \quad C_2 \quad C_3 \quad C_4 \quad C_5 \quad C_6\}$ are the unknown constants

$$\begin{Bmatrix} \hat{u}(x) \\ \hat{w}(x) \\ \hat{\theta}(x) \end{Bmatrix} = [R] \begin{bmatrix} e^{-ik_1 x} & 0 & 0 & 0 & 0 & 0 \\ 0 & e^{-ik_1(L-x)} & 0 & 0 & 0 & 0 \\ 0 & 0 & e^{-ik_2 x} & 0 & 0 & 0 \\ 0 & 0 & 0 & e^{-ik_2(L-x)} & 0 & 0 \\ 0 & 0 & 0 & 0 & e^{-ik_3 x} & 0 \\ 0 & 0 & 0 & 0 & 0 & e^{-ik_3(L-x)} \end{bmatrix} \begin{Bmatrix} C_1 \\ C_2 \\ C_3 \\ C_4 \\ C_5 \\ C_6 \end{Bmatrix} \tag{6.6}$$

Applying boundary conditions at two nodes, *i.e.* $x = 0 \ \ and \ \ x = L$

$$\begin{Bmatrix} \hat{u}_1 \\ \hat{w}_1 \\ \hat{\theta}_1 \end{Bmatrix} = [R] \begin{bmatrix} 1 & 0 & 0 & 0 & 0 & 0 \\ 0 & e^{-ik_1 L} & 0 & 0 & 0 & 0 \\ 0 & 0 & 1 & 0 & 0 & 0 \\ 0 & 0 & 0 & e^{-ik_2 L} & 0 & 0 \\ 0 & 0 & 0 & 0 & 1 & 0 \\ 0 & 0 & 0 & 0 & 0 & e^{-ik_3 L} \end{bmatrix} \begin{Bmatrix} C_1 \\ C_2 \\ C_3 \\ C_4 \\ C_5 \\ C_6 \end{Bmatrix} \tag{6.7}$$

$$\begin{Bmatrix} \hat{u}_1 \\ \hat{w}_1 \\ \hat{\theta}_1 \end{Bmatrix} = [R][\Theta_{D1}]\{C\} = [T_{11}]\{C\} \tag{6.8}$$

$$\begin{Bmatrix} \hat{u}_2 \\ \hat{w}_2 \\ \hat{\theta}_2 \end{Bmatrix} = [R] \begin{bmatrix} e^{-ik_1 L} & 0 & 0 & 0 & 0 & 0 \\ 0 & 1 & 0 & 0 & 0 & 0 \\ 0 & 0 & e^{-k_2 L} & 0 & 0 & 0 \\ 0 & 0 & 0 & 1 & 0 & 0 \\ 0 & 0 & 0 & 0 & e^{-ik_3 L} & 0 \\ 0 & 0 & 0 & 0 & 0 & 1 \end{bmatrix} \begin{Bmatrix} C_1 \\ C_2 \\ C_3 \\ C_4 \\ C_5 \\ C_6 \end{Bmatrix} \tag{6.9}$$

$$\begin{Bmatrix} \hat{u}_2 \\ \hat{w}_2 \\ \hat{\theta}_2 \end{Bmatrix} = [R][\Theta_{D2}]\{C\} = [T_{12}]\{C\} \tag{6.10}$$

Combining equations (6.8) and (6.10), the nodal displacement vector can be written as

$$\{\hat{U}\} = \begin{Bmatrix} \hat{u}1 \\ \hat{w}1 \\ \hat{\theta}_1 \\ \hat{u}2 \\ \hat{w}2 \\ \hat{\theta}_2 \end{Bmatrix} = \begin{bmatrix} T_{11} \\ T_{12} \end{bmatrix} \{C\} = [T_1]\{C\} \tag{6.11}$$

Next,Similarly boundary conditions applying to the nodal force $\hat{F}(x)$,shear force $\hat{V}(x)$ and moment $\hat{M}(x)$ are given in equations (5.37), (5.79) and (5.80).

$$\hat{F}_j = EA\frac{d\hat{u}_j}{dx} \tag{6.12}$$

Equation (6.1) substituting into equation (6.12), we have;

$$\hat{F}(x) = \text{EA}\left(-ik_1c_1e^{-ik_1x} + ik_1c_2e^{-ik_1(L-x)}\right) \tag{6.13}$$

$$\hat{V}(x) = -EI\left(ik_2^3C_1e^{-ik_2x} - ik_2^3C_2e^{-ik_2(L-x)} - ik_3^3C_3e^{-ik_3x} + ik_3^3C_4e^{-ik_3(L-x)}\right) \tag{6.14}$$

$$\hat{M}(x) = EI\left(-k_2^2C_1e^{-ik_2x} - k_2^2C_2e^{-ik_2(L-x)} - k_3^2C_3e^{-k_3x} - k_3^2C_4e^{-k_3(L-x)}\right) \tag{6.15}$$

The above equations are writing in matrix form as

$$\begin{Bmatrix} \hat{F}(x) \\ \hat{V}(x) \\ \hat{M}(x) \end{Bmatrix} = \left[R^{1'}\right] \begin{bmatrix} e^{-ik_1x} & 0 & 0 & 0 & 0 & 0 \\ 0 & e^{-ik_1(L-x)} & 0 & 0 & 0 & 0 \\ 0 & 0 & e^{-ik_2x} & 0 & 0 & 0 \\ 0 & 0 & 0 & e^{-ik_2(L-x)} & 0 & 0 \\ 0 & 0 & 0 & 0 & e^{-ik_3x} & 0 \\ 0 & 0 & 0 & 0 & 0 & e^{-ik_3(L-x)} \end{bmatrix} \begin{Bmatrix} C_1 \\ C_2 \\ C_3 \\ C_4 \\ C_5 \\ C_6 \end{Bmatrix} \tag{6.16}$$

Applying boundary conditions at two nodes i.e. $x = 0 \ and \ x = L$

$$\begin{Bmatrix} \hat{F}_1 \\ \hat{V}_1 \\ \hat{M}_1 \end{Bmatrix} = [R^1][\Theta_{D1}]\{C\} = [T_{21}]\{C\} \tag{6.17}$$

$$\begin{Bmatrix} \hat{F}_2 \\ \hat{V}_2 \\ \hat{M}_2 \end{Bmatrix} = [R^1][\Theta_{D2}]\{C\} = [T_{22}]\{C\} \tag{6.18}$$

Combining equations (6.17) and (6.18), the nodal force vector can be written as

$$\{\hat{F}^e\} = \begin{Bmatrix} \hat{F}_1 \\ \hat{V}_1 \\ \hat{M}_1 \\ \hat{F}_2 \\ \hat{V}_2 \\ \hat{M}_2 \end{Bmatrix} = \begin{bmatrix} T_{21} \\ T_{22} \end{bmatrix}\{C\} = [T_2]\{C\} \tag{6.19}$$

Elimating $\{C\}$ from equations (6.11) and (6.19), the nodal displacement vector can be related to the nodal force vector as

$$\{\hat{F}^e\} = [T_2][T_1]^{-|}\{\hat{U}\} \tag{6.20}$$

$$\{\hat{F}^e\} = [\hat{k}_e]\{\hat{U}\} \tag{6.21}$$

where, $[\hat{k}_e]$ is the elemental dynamic stiffness matrix.

The above equation can be solved to obtain the nodal displacement vector $\{\hat{U}\}$ for known nodal forces.

$$\{\hat{U}\} = \{\hat{F}^e\}[\hat{k}_e]^{-|} \tag{6.25}$$

$\{\hat{U}\}$ can be substituted into equation (6.11) to derive the constant $\{C\}$ as

$$\{C\} = \{\hat{U}\}[T_1]^{-|} \tag{6.26}$$

After knowing constant $\{C\}$, it can be substituted into equation (6.3) to obtain the $\hat{u}(x)$ at any arbitrary points (XS) on the rod. i.e. putting $x = XS$

CHAPTER-7

RESULTS & DISCUSSION

The wave propagation analysis is done for cantilever Extended Euler-Bernoulli beam with Young's modulus $E = 70 \times 10^9\, N/m^2$ and denity $\rho = 2.7 \times 10^3\, kg/m^3$. The Extended Euler-Bernoulli beam is fixed at one end and an impulse load shown in figure 7 is applied axial and transverse at the free end as shown in figures 10 and 11. The load is of unit amplitude and duration of 50 μs with a frequency content of 44 KHz. The length, width and depth of Extended Euler-Bernoulli beam under axial impulse load taken as $L = 0.508\, m, b = 0.0254\, m\, and\, d = 0.000254\, m$. For Extended Euler-Bernoulli beam under transverse impulse load, elastic properties and dimensions are same as the Extended Euler-Bernoulli beam under axial impulse load except the length $L = 0.254\, m$. The wavelet basis function used has an order of Daubechies N=22.

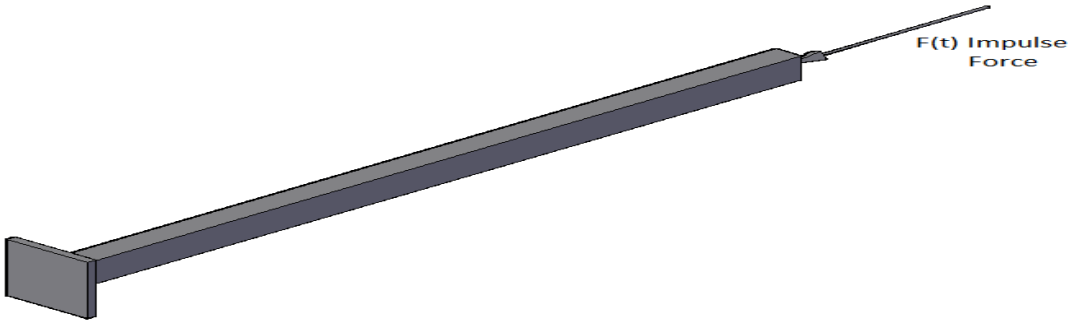

FIGURE 10 Aluminum cantilever rod element

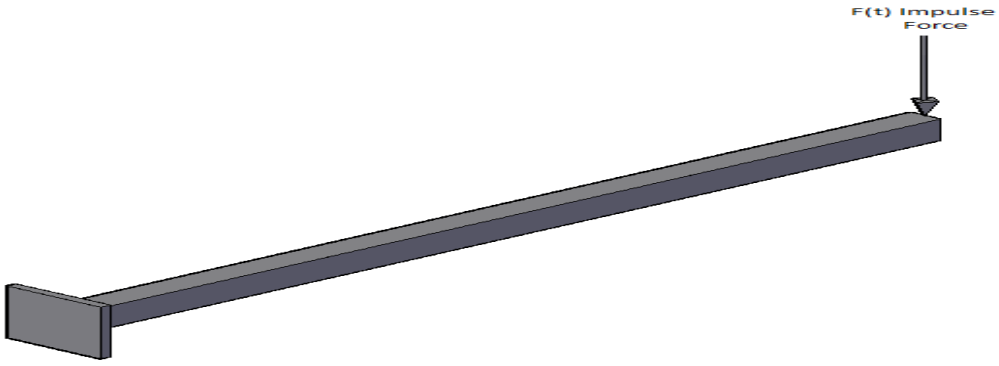

FIGURE 11 Aluminum cantilever beam element

7.1 Results of spectral finite element formulation

TABLE 4: wave numbers (k):

s.no	Wave numbers (k)
1	-0.0000 – 2397.1i
2	0.0000 + 2397.1i
3	421.3 - 0.0000i
4	-421.3 + 0.0000i
5	2397.1 - 0.0000i
6	-2397.1 + 0.0000i

Amplitude ratio matrix [R]

$$[R]=\begin{bmatrix} 0 & 0 & -1 & -1 & 0 & 0 \\ -1 & -1 & 0 & 0 & 1 & 1 \\ 2397.1-0.00i & -2397.1+0.00i & 0 & 0 & -0.00-2397.1i & 0.00+2397.1i \end{bmatrix}$$

$$[\theta_{D1}]=\begin{bmatrix} 1.00 & 0 & 0 & 0 & 0 & 0 \\ 0 & 0.00+0.00i & 0 & 0 & 0 & 0 \\ 0 & 0 & 1.00 & 0 & 0 & 0 \\ 0 & 0 & 0 & 0.98-0.20i & 0 & 0 \\ 0 & 0 & 0 & 0 & 1.00 & 0 \\ 0 & 0 & 0 & 0 & 0 & 0.83+0.56i \end{bmatrix}$$

$$T_{11}=\begin{bmatrix} 0 & 0 & -1 & -1+0.2i & 0 & 0 \\ -1 & -0.00-0.00i & 0 & 0 & 1 & 0.8+0.6i \\ 2397.1-0.00i & -0.00-0.00i & 0 & 0 & -0.00-2397.1i & -1339.5+1983.4i \end{bmatrix}$$

$$[\theta_{D2}]=\begin{bmatrix} 0.00+0.00i & 0 & 0 & 0 & 0 & 0 \\ 0 & 1.00 & 0 & 0 & 0 & 0 \\ 0 & 0 & 0.98-0.2\text{i} & 0 & 0 & 0 \\ 0 & 0 & 0 & 1.00 & 0 & 0 \\ 0 & 0 & 0 & 0 & 0.83+0.56\text{i} & 0 \\ 0 & 0 & 0 & 0 & 0 & 1.00 \end{bmatrix}$$

$$[T_{12}]=\begin{bmatrix} 0 & 0 & -1+0.2\text{i} & -1 & 0 & 0 \\ -0.00-0.00 & -1 & 0 & 0 & 0.8+0.6\text{i} & 1 \\ 0.00+0.00\text{i} & -2397.1+0.00\text{i} & 0 & 0 & 1339.5-1983.4\text{i} & 0.00+2397.1\text{i} \end{bmatrix}$$

$$[T_1]=\begin{bmatrix} 0 & 0 & -1 & -1+0.2\text{i} & 0 & 0 \\ -1 & -0.00-0.00\text{i} & 0 & 0 & 1 & 0.8+0.6\text{i} \\ 2397.1-0.00\text{i} & -0.00-0.00\text{i} & 0 & 0 & -0.00-2397.1\text{i} & -1339.5+1983.4\text{i} \\ 0 & 0 & -1+0.2\text{i} & -1 & 0 & 0 \\ -0.00-0.00\text{i} & -1 & 0 & 0 & 0.8+0.6\text{i} & 1 \\ 0.00+0.00\text{i} & -2397.1+0.00\text{i} & 0 & 0 & 1339.5-1983.4\text{i} & 0.00+2397.1\text{i} \end{bmatrix}$$

$$[T_2]=$$

$$\begin{bmatrix} 0 & 0 & 0+190\times10^{6}i & -38\times10^{6}-186\times10^{6}i & 0 & 0 \\ -0-10\times10^{3}i & 0-0\text{i} & 0 & 0 & -0-10\times10^{3}i & 10\times10^{3}-10\times10^{3}i \\ -10\times10^{3}+0i & -0-0\text{i} & 0 & 0 & -10\times10^{3}+0i & -10\times10^{3}-10\times10^{3}i \\ 0 & 0 & -38\times10^{6}-186\times10^{6}i & 0+190\times10^{6}i & 0 & 0 \\ -0+0\text{i} & 0+10\times10^{3}i & 0 & 0 & -10\times10^{3}-10\times10^{3}i & 0+10\times10^{3}i \\ 0+0i & 10\times10^{3}-0i & 0 & 0 & 10\times10^{3}+10\times10^{3}i & 10\times10^{3}-0i \end{bmatrix}$$

Elemental dynamics stiffness matrix k_e

$$\begin{bmatrix} -0.91\times10^{9}-2.51\times10^{6}i & 0 & 0 & 0.93\times10^{9}+2.45\times10^{6}i & 0 & 0 \\ 0 & 0.01\times10^{9}-80\times10^{3}i & -10\times10^{3}-0i & 0 & -0.04\times10^{9}-40\times10^{3}i & 20\times10^{3}+0i \\ 0 & -10\times10^{3}-0i & -0-0\text{i} & 0 & -20\times10^{3}-0i & 0+0\text{i} \\ 0.93\times10^{9}+2.45\times10^{6}i & 0 & 0 & -0.91-2.51\times10^{6}i & 0 & 0 \\ 0 & -0.04\times10^{9}-40\times10^{3}i & -20\times10^{3}-0i & 0 & 0.01\times10^{9}-80\times10^{3}\text{i} & 10\times10^{3}+0i \\ 0 & 20\times10^{3}+0i & 0+0\text{i} & 0 & 10\times10^{3}+0i & -0-0\text{i} \end{bmatrix}$$

After applying boundary conditions for cantilever beam

$$[k_e]=\begin{bmatrix} -0.910\times10^{9} & 0 & 0 \\ 0 & -0+10\times10^{3}i & 0-0\text{i} \\ 0 & 10\times10^{3}+0i & -0-0\text{i} \end{bmatrix}$$

7.2 Response of Extended Euler-Bernoulli aluminum beam under axial impulse load

Wave propagation analysis is done for an Extended Euler-Bernoulli aluminum beam under axial impulse load. The Extended Euler-Bernoulli aluminum beam is fixed at one end and an axial impulse load as shown in figure 7 is applied at the free end. Figure 13 shows the tip longitudinal velocity in undamped ($\eta = 0$). The wavelet basis function used has an order of Daubechies N= 22.and the sampling rate $\Delta t = 1, 2, and\ 4\ \mu s$ for a time windows $512\ \mu s$.

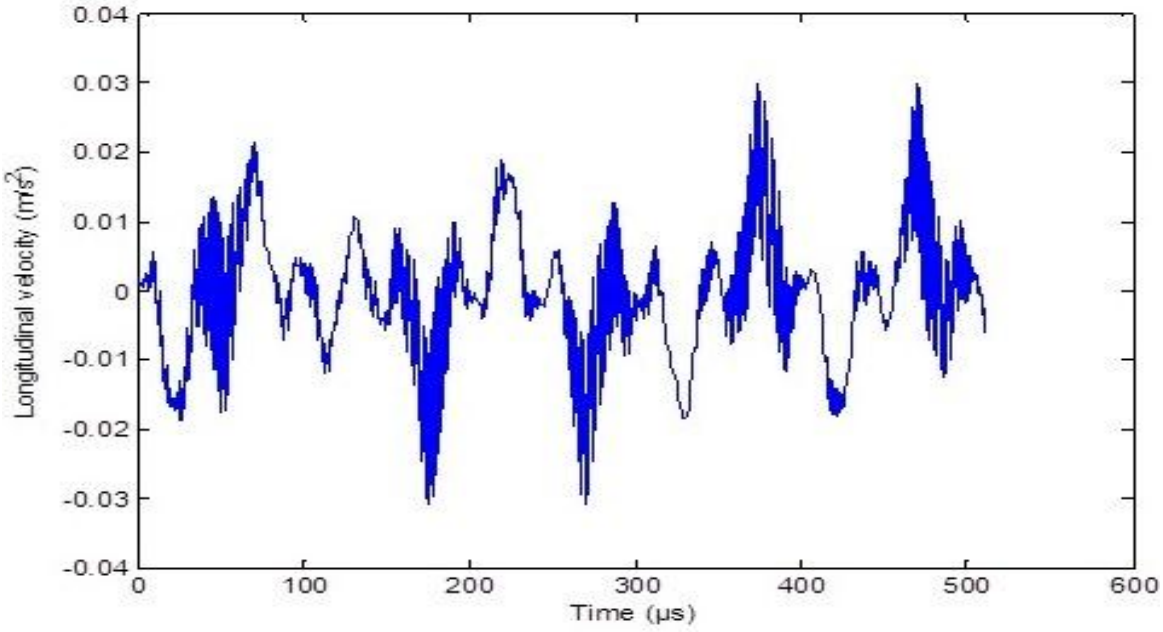

$\Delta t = 1\ \mu s$

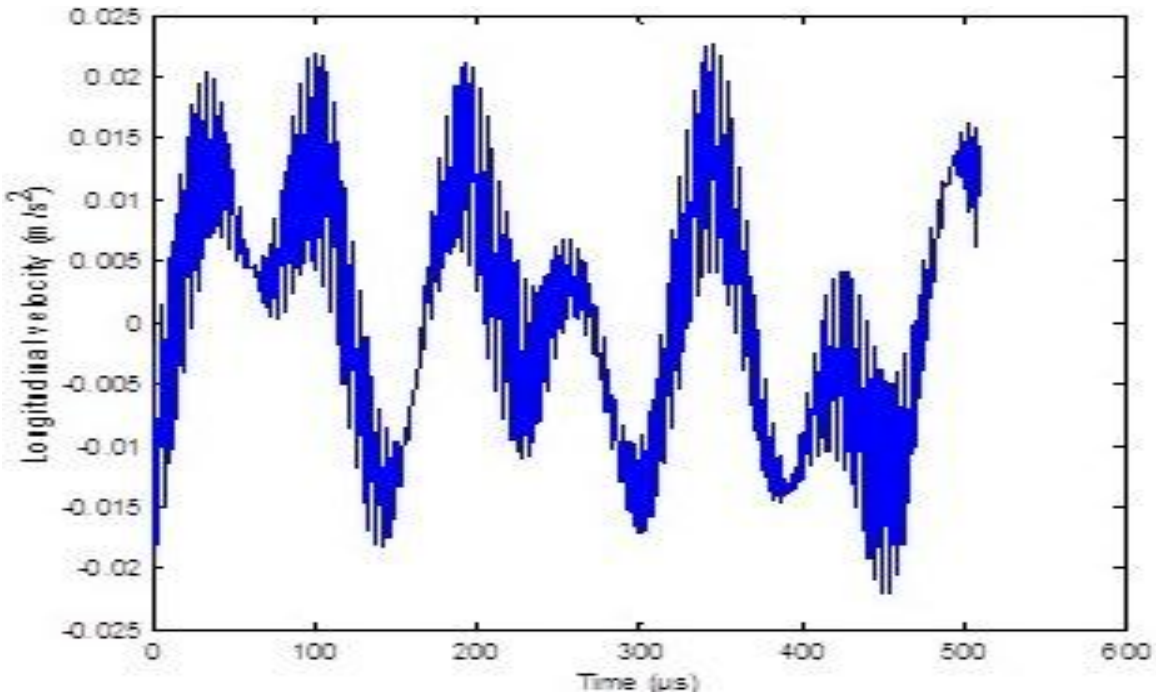

$\Delta t = 2\ \mu s$

FIGURE 12: Longitudinal tip velocity Extended Euler-Bernoulli aluminum beam under axial impact load simulated with different time interval $\Delta t = 1\ and\ 2$ and order of Daubechies N=6

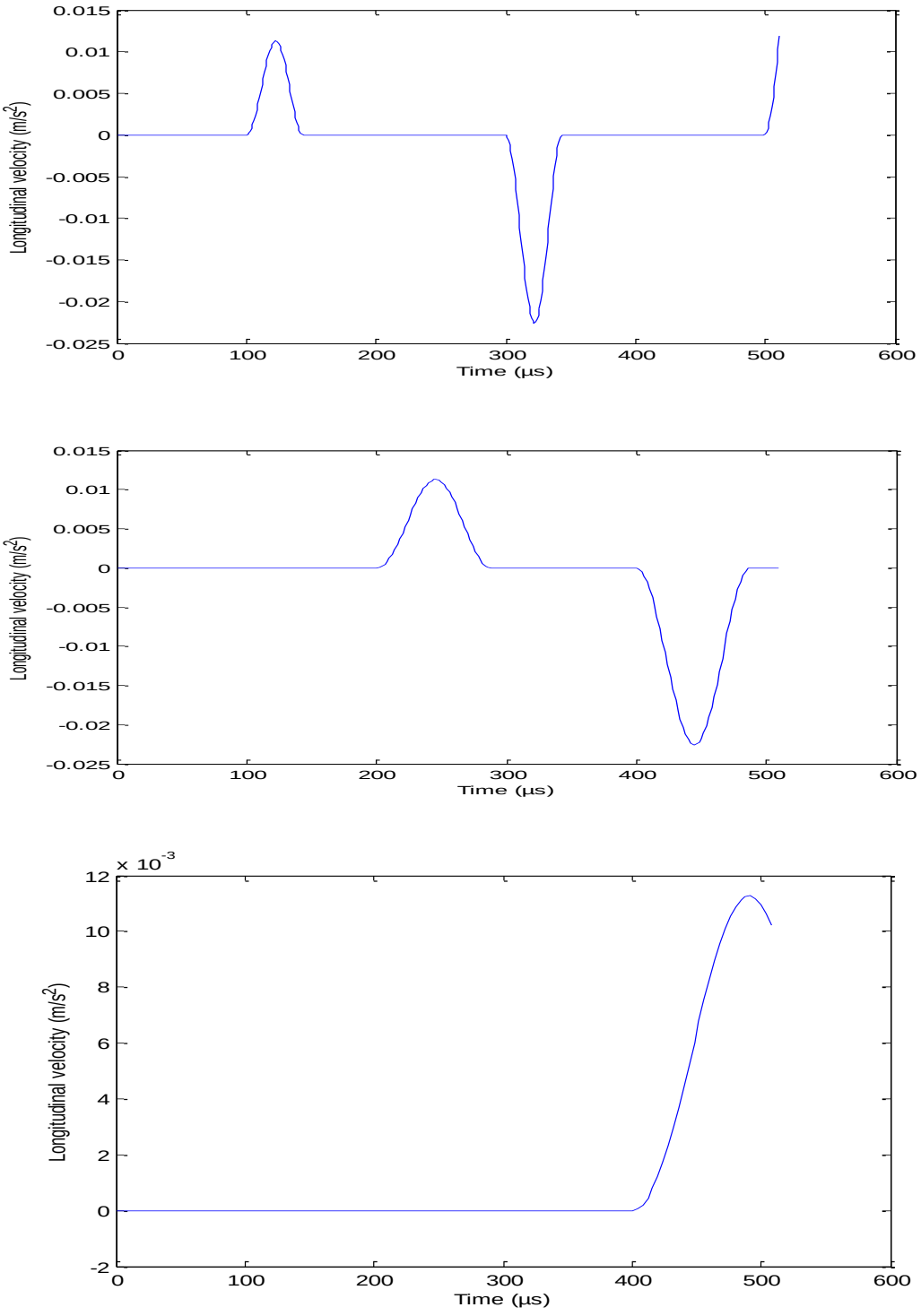

FIGURE 13: Longitudinal tip velocity in Extended Euler-Bernoulli aluminum beam under axial impact load simulated with different time intervals i.e. $\Delta t = 1, 2\ and\ 4$ and order of Daubechies N=22

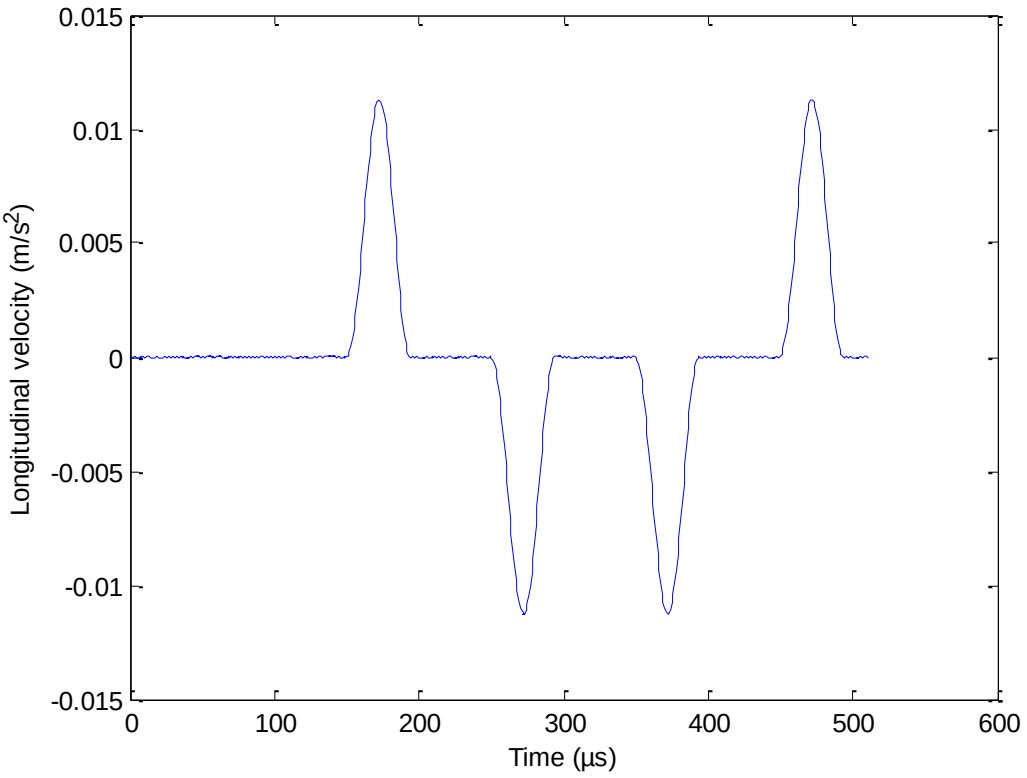

FIGURE 14: Longitudinal velocity at midpoint of Extended Euler-Bernoulli aluminum beam under axial impact load at tip simulated with time interval $\Delta t = 1$ and order of Daubechies N=22

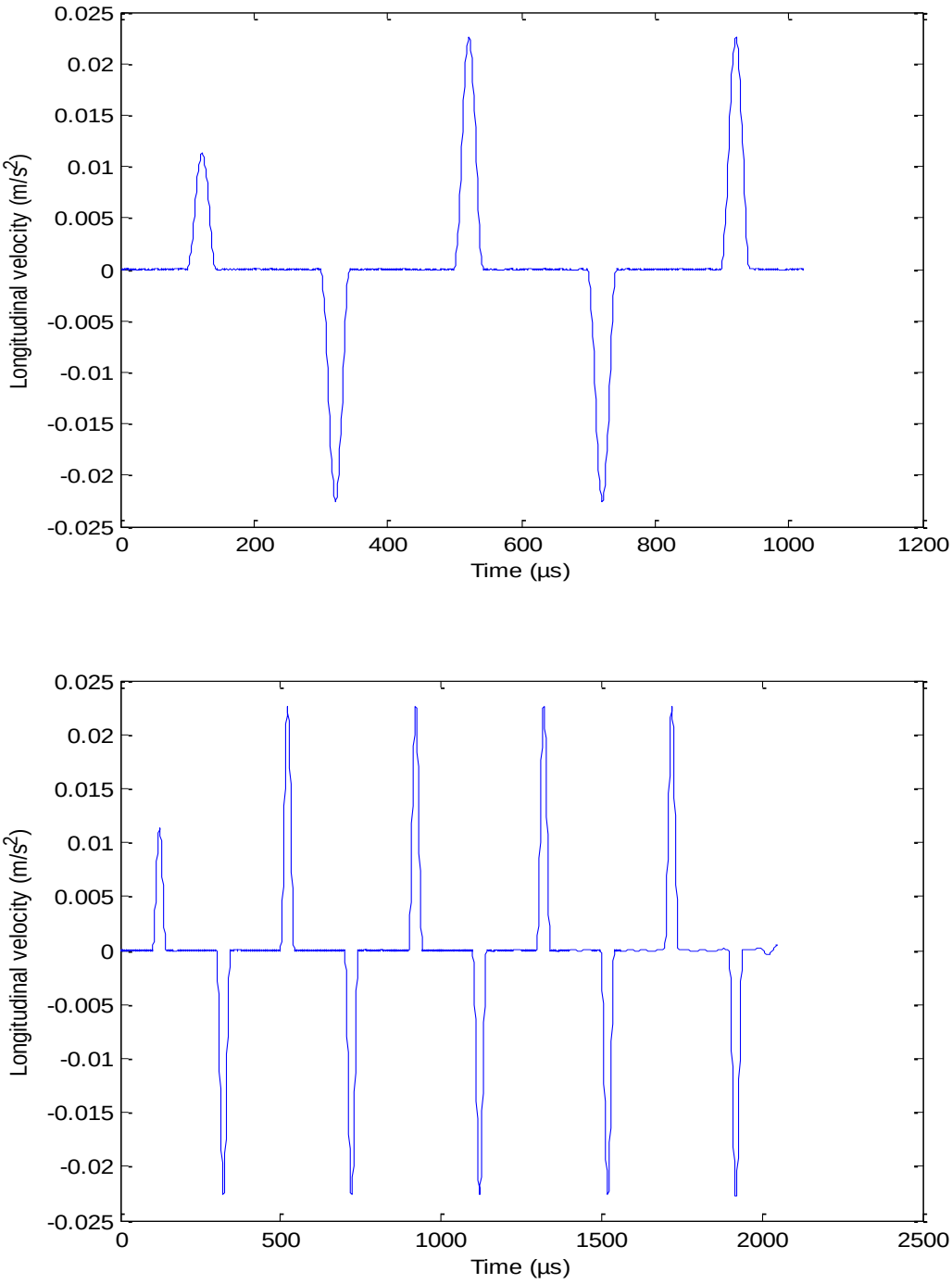

FIGURE 15: Longitudinal tip velocity in Extended Euler-Bernoulli aluminum beam under axial impact load at tip for time window (a) 1024 (b) 2048 for order of Daubechies N=22.

7.3 Response of Extended Euler-Bernoulli aluminum beam under transverse impulse load

The flexural wave propagation in Extended Euler-Bernoulli aluminum beam under transverse impulse load. The beam is fixed at one end and an impulse load as shown in figure 7 applied at the free end of the beam. Figure16 shows the tip transverse velocity in undamped ($\eta = 0$). The wavelet basis function used has an order of Daubechies N=22.and the sampling rate $\Delta t = 1\ \mu s$ for a time window $2048\ \mu s$.

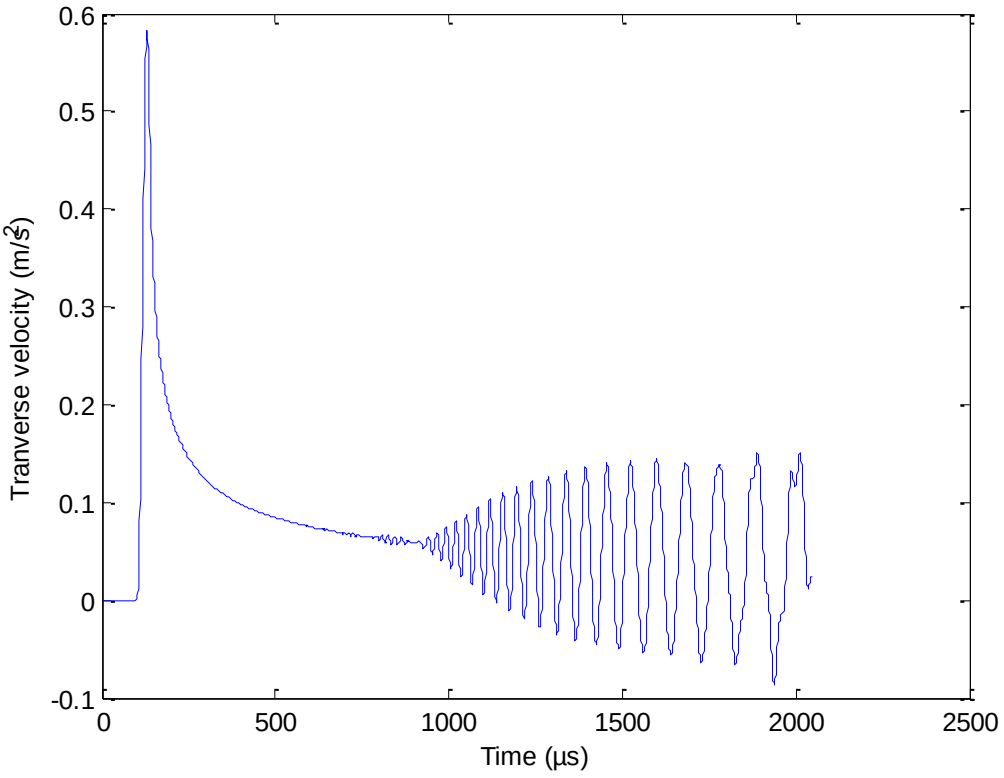

FIGURE 16: Transverse tip velocity in Extended Euler-Bernoulli aluminum beam due to tip impact load simulated with time interval $\Delta t = 1$ and order of Daubechies N=22

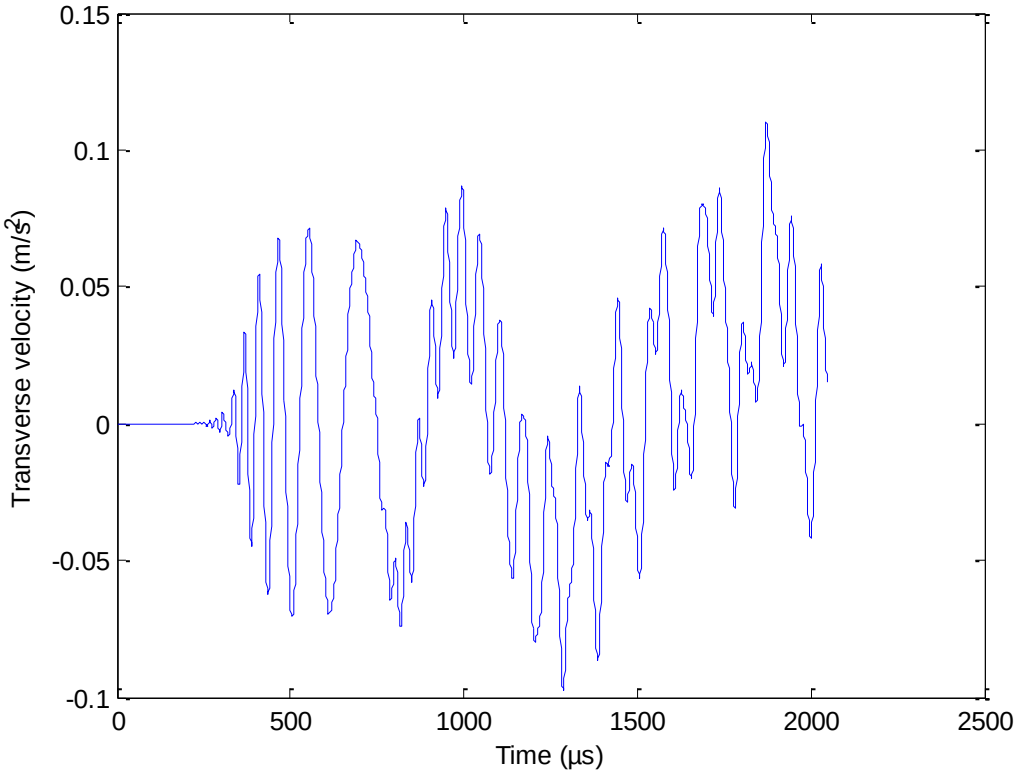

FIGURE 17: Transverse velocity at midpoint of Extended Euler-Bernoulli aluminum beam due to tip impact load simulated with time interval $\Delta t = 1$ and order of Daubechies N=22

CHAPTER ~ 8

Conclusion

The formulation and validation of wavelet spectral element for simulation of wave propagation in an Extended Euler-Bernoulli aluminum beam has been presented.

1 Spectral element method proves to be an efficient alternative to finite element analysis of wave propagation problems and decreases the computational cost substantially.

2 The novelty of the spectral element developed is that it uses wavelet transform to reduce the partial differential equations to ordinary differential equations unlike the solution which is used in the spectral finite element formulation.

3 The finite element method analysis involves a large number of elements for the solution whereas wavelet spectral finite element method involves only a single element for the solution.

4 When the time window is increased there is undulation in the axial velocities of the Extended Euler-Bernoulli aluminum beam under axial impulse load.

5 When the time interval is increased i.e. when the number of sampling points is decreased the solution has got more errors.

6 When the order of Daubechies increased the error in the solution decreased.

7 In case of Extended Euler-Bernoulli aluminum beam under axial impulse load, the velocity is non-dispersive when as in case of beam under transverse impulse load it is dispersive.

References

[1] **Amaratunga, K., Williams, J. R., Qian, S.and Weiss, J**. Wavelet based Green's function approach to 2D PDE's. *Engineering Computation,* **10 (4),** 349–367, 1993.

[2] **Amaratunga, K. and Williams, J. R**. Time integration using wavelets. In: Proceedings of SPIE, *Wavelet Application for Dual Use*, **2491**, Orlando, FL, 894–902, 1995.

[3] **Amaratunga, K.** and **Williams, J. R**. Wavelet–Galerkin solution of boundary value problems. *Archives of Computational Methods in Engineering*, **4 (3)**, 243–285, 1997.

[4] **Beylkin, G**. On the representation of operators in bases of compactly supported Wavelets. *SIAM Journal of Numerical Analysis*., **6(6),** 1716-1740, 1992.

[5] **Bertoluzza, S. and Naldi, G**. Some remarks on wavelet interpolation. *Computational and Applied Mathematics*, **13(1),** 13-32, 1994.

[6] **Bathe, K. J**. Finite element procedures. Prentice Hall, NJ, 1996.

[7] **Beskos, D. E.** Boundary element method in dynamics analysis part II (1986-1996). *Applied Mechanics Review*, **50**, 149-197, 1997.

[8] **Batra, R. C.** and **Ching, H. K**. Analysis of elasto dynamics deformations near a crack/notch tip by the meshless local Petrov-Galerkin (MLPG) method. *Computer Modeling in Engineering and Science* (CMES), **3(6),** 717-730, 2002.

[9] **Bajaba, N. S. and Alnefaie, K. A.** Multiple damage detection in structures using wavelet transforms. *Emirates Journal for Engineering Research*, **10 (1),** 35-40, 2005.

[10] **Canuto, C., Hussaini, M. Y., Quarteroni**, **A**. and **Zang, T. A**. *Spectral Method in Fluid Dynamics*, Springer Verleg, 1988.

[11] **Cohen, A**. Bi-orthogonal wavelets. Wavelets: A tutorial in theory and applications. C. K. Chui, ed., Academic, San Diego, 123-152, 1992.

[12] **Cohen, A., Daubechies, I**. **and Feauvean, J. C.** Bi-orthogonal bases of compactly Supported wavelets. *Communications in Pure and Applied Mechanics*, **45**, 485-560, 1992.

[13] **Daubechies, I.** Orthonormal bases of compactly supported wavelets. *Comm. In Pure and Applied Mathematics*, **41**, 906-966, 1988.

[14] **Donoho, D. L**. Interpolating wavelet transforms. Technical Report, Department of Statistics, Stanford University, 1992.

[15] **Daubechies, I**. *Ten Lectures on Wavelets*, SIAM, Philadelphia, 1992.

[16] **Doyle, J. F**. Wave propagation in structures. Springer, New York, 1999.

[17] **Dahmen, W**. Wavelet methods for PDEs some recent developments. *Journal of Computational and Applied Mathematics*, **128(1–2)**, 133–185, 2001.

[18] **Graff, K. F**. Wave motions in elastic solids. Ohio State University Press, 1975.

[19] **Grossmann, A. and Morlet, J**. Decomposition of Hardy functions in to square Integrable wavelets of constant shape. *SIAM Journal of Mathematical Analysis*, **15**, 723-736, 1984.

[20] **Glowinski, R., Lawton, W., Ravachol, M.** and **Tanenbaum, E**. Wavelet solution of linear and nonlinear elliptic, parabolic and hyperbolic problems in one space dimension. In: Proceedings of the 9th International Conference on Numerical Methods in *Applied Sciences and Engineering*, SIAM, Philadelphia, 1990.

[21] **Graps, A**. An Introduction to Wavelets. *Computational Science and Engineering*, **2(2),** 1995.

[22] **Gopalakrishnan, S., Chakraborty, A. and Mahapatra, D**.**Y**. Spectral finite Element method: Wave propagation, diagnostics and control in an-isotropic and In-homogeneous structures. Springer, 2007.

[23] **Gurley, K. and Kareem, A**. Applications of Wavelet Transforms in Earthquake, Wind and Ocean Engineering. *Department of Civil Engineering and Geological Sciences*, University of Notre Dame, Notre Dame, IN, 46556

[24] **Hu, F. Q., Hussaini, M. Y. and Rasetarinera, P.** An analysis of the discontinuous Galerkin method for wave propagation methods. *Journal of Computational Physics*, **151(2)**, 921-946, 1999.

[25] **Hong, T. K., Kennett, B. L. N**. On a wavelet based method for the numerical simulation of wave propagation. *Journal of Computational Physics*, **183,** 577-622, 2002.

[26] **Han, J. G., Ren, W. X. and Huang, Y.** A spline wavelet finite-element method in structural mechanics. *International Journal for Numerical Methods in Engineering*, **66**,166–190, 2006.

[27] **Hariharan, G**. Solving finite length beam equation by the Haar wavelet method. *International Journal of Computer Applications*, 9(1), 27-34, 2010.

[28] **Jameson, L**. On the wavelet based differentiation matrix. Journal of Scientific Computing, **8(3),** 1993.

[29] **Joly, P., Maday, Y.** and **Perrier, V**. Towards a method for solving partial differential equations by using wavelet packet bases. *Computer Methods in Applied Mechanics and Engineering*, **116 (2),** 193–202, 1994.

[30] **Kaiser, G**. *A Friendly Guide to Wavelets*, Birkhauser, Boston, 44-45, 1994.

[31] **Kumar, B. V. R** and **Mehra, M**. *International Journals of Computational Methods*, **2**, 75–97, 2005.

[32] **Kozbial, T.** Application of Daubechies wavelets approximation to plate bending. *Proc .Appl. Math. Mech*, **6**, 231–232, 2006.

[33] **Khatam, H., Golafshani, A. A., Beheshti-Aval, S. B. and Noori, M**. Harmonic class loading for damage identification in beams using wavelet analysis. *Structural Health Monitoring*, **6(1),** 67-80, 2007.

[34] **Lancaster, P.** Lambda matrices and vibrating systems. Pergamon Press, 1966.

[35] **Latto, A., Resnikoff, H.L. and Tanenbaum**, **E**. The evaluation of connection Coefficients of compactly supported wavelets. Cambridge-USA, 1999.

[36] **Loutridis, S., Douk, E. and Trochidis, A**. Crack identification in double-cracked beams using wavelet analysis. *Journal of Sound and Vibration*, **277**, 1025–1039, 2004.

[37] **Law, S. S., Wu, S. Q. and Shi, Z. Y.** Moving Load and Prestress Identification Using Wavelet-Based Method. *Journal of Applied Mechanics*, **75**, 2008.

[38] **Lee, U. and Kwon, K**. Spectral element modeling of the thermally induced vibration of an axially moving plate. Journal of Achievements in Materials and Manufacturing Engineering, **26(1),** 65-72, 2008.

[39] **Morlet, J., Arens, G., Fourgeau, I. and Giard, D.** Wave propagation and sampling theory. *Geophysics*, **47**, 203-236, 1982.

[40] **Morlet, J**. Sampling theory and wave propagation. In C. H. Chen (ed.), NATO ASI Series, Issues in Acoustic Signal/Image Processing and Recognition, Springer, Berlin, **1**, 233-261, 1983.

[41] **Mansur, W. J**. *A time stepping technique to solve wave propagation problems using the boundary element method*. PhD thesis, Southampton University, 1983.

[42] **Mallat, S. G.** Multi-resolution approximation and wavelets. Preprint GRASP Lab., Department of Computer and Information Science. University of Pennsylvania, 1986.

[43] **Meyer,Y**. Principed' incertitude, bases hilbertiennes et albebresd' operateurs'. Seminaire Bourbaki, 662, 1987.

[44] **Ma, J., Xue, J., Yang, S. and He, Z**. A study of the construction and application of a Daubechies wavelet-based beam element. *Finite Elements in Analysis and Design*, 39, 965–975, 2003.

[45] **Morton, K.** and **Mayers, D**. *Numerical Solution of Partial Differential Equations*, Cambridge University Press, 2005.

[46] **Mehra, M.** and **Kumar, B. V. R**. *Communications in Numerical Methods in Engineering*, **21**, 313–326, 2005.

[47] **Mitra, M. and Gopalakrishnan, S**. Spectrally formulated wavelet finite element for Wave propagation and impact force identification in connected 1-D waveguides. *International journal of solids and structures*, **42**, 4695-4721, 2005.

[48] **Mitra, M. and Gopalakrishnan, S**. Extraction of wave characteristics from wavelet-based spectral finite element formulation. *Mechanical Systems and Signal Processing*, 20, 2046–2079, 2006.

[49] **Mitra, M. and Gopalakrishnan, S.** Wavelet Based 2-D Spectral Finite Element Formulation for Wave Propagation Analysis in Isotropic Plates. *CMES*, **15(1)**, 49-67, 2006.

[50] **Mitra, M. and Gopalakrishnan, S.** Wavelet based spectral finite element modeling and detection of de-lamination in composite beams. *Proc. R. Soc A*, **462**, 1721–1740, 2006.

[51] **Mira Mitra.and Gopalakrishan, S.** Wavelet Methods For Dynamical Problems With Application to Metallic, Composites, and Nano-Composites Structures.

[52] **Mitra, M. and Gopalakrishnan, S**. Vibrational characteristics of single-walled Carbon-nanotube: Time and frequency domain analysis. *Journal of Applied Physics*, **101**,114320, 2007.

[53] **Mitra, M. and Gopalakrishnan, S**. Wavelet spectral element for wave propagation Studies in pressure loaded axis symmetric cylinders. *Journal of mechanics of Materials and Structures*, **2(4),** 753-772, 2007.

[54] **Mitra, M., Gopalakrishnan, S., Ruzzene, M., Apetre, N. and Hanagud, S**. Perturbation technique for wave propagation analysis in a notched beam using wavelet spectral element modeling. *Journal of Mechanics of Materials and Structures*. **3 (4),** 2008.

[55] **Mitra, M. and Gopalakrishnan, S**. Wave propagation analysis in anisotropic plate using wavelet spectral element approach. *Journal of Applied Mechanics***, 75**, 014504, 2008.

[56] **Mehra, M.***AIP Conference Proceedings*, **1146**, 241–252, 2009.

[57] **Mahmoud, M. and Taha, R.** A Neural-Wavelet Technique for Damage Identification in the ASCE Benchmark Structure Using Phase II Experimental Data**.** *Hindawi Publishing Corporation Advances in Civil Engineering*, 2010.

[58] **Mehra, M., Patel, N. and Kumar, R**. Comparison between different numerical methods for discretization of PDEs a short review. *Indian Institute of Technology Delhi, HauzKhas, New Delhi–110116, India.*

[59] **Narayanan, G. V.** and **Beskos, D. E**. Use of dynamic influence coefficients in forced vibration problems with the aid of fast Fourier transform. *Computers and Structures*, **9,** 445-450, 1978.

[60] **Press et al, W**. *Numerical Recipes in FORTRAN*, Cambridge University Press, New York, 498-499, 1992.

[61] **Park, S. H.** and **Tassoulas, J. L**. A discontinuous Galerkin method for transient analysis of wave propagation in unbounded domains. *Computer Method in Applied Mechanics and Engineering*, **191(36),** 3983-4011, 2002.

[62] **Rucka, M. and Wilde, K**. Application of continuous wavelet transform in vibration based damage detection method for beams and plates. *Journal of Sound and Vibration*, **297**, 536–550, 2006.

[63] **Sneddon, I.** Fourier transforms. McGraw Hill, New York, 1951.

[64] **Stromberg, J. O**. A modified Franklin system and higher order spline system on r^nas unconditional bases for hardy spaces. Conf.in Honour of A. Zgmund, Wadsworth Mathematics Series, **2**, 1982.

[65] **Shorr, B. F.** *The wave finite element method.* Springer, Berlin, 2004.

[66] **Sonekar, P. and Mitra, M**. A wavelet-based model of one-dimensional periodic structure for wave-propagation analysis. *Proc. R. Soc. A,* **466**, 263-281, 2010.

[67] **Trefethen, L. N.** *Spectral Methods in MATLAB*, SIAM, Philadelphia, PA, 2000.

[68] **Vonesch, C.,Blu, T. and Unser, M**. Generalized Daubechies Wavelet Families. *IEEE Transactions on Signal Processing*, **55(9),** 4415-4429, 2007.

[69] **Vampa, V. and Maria T. Martin and Lilliam Alvarez Diaz**. A Daubechies wavelet beam element **.***Mechanics Computational*, **26,** 654-666**,** 2007.

[70] **Williams, J. R. and Amaratunga, K.**A discrete wavelet transform without edge effects using wavelet extrapolation. *Journal of Fourier Analysis and Applications*, **3(4),** 435-449, 1997.

[71] **Xiang, J. W. and Liang, M**. Multiple crack identification using frequency measurement. *World Academy of Science, Engineering and Technology*, **76**, 2011.

[72] **Yaghin, M. A. L. and Hesari, M. A**. Using wavelet analysis in crack detection at the arch concrete dam under frequency analysis with FEM. *World Applied Sciences*, **3 (4),** 691-704, 2008.

[73] **Zhou, Y. H. and Zhou, J.** A modified wavelet approximation of deflections for solving PDEs of beams and square thin plates. *Finite Elements in Analysis and Design*, **44**, 773– 783, 2008.